Search for new particles decaying to a jet and an emerging jet

The CMS collaboration

E-mail: cms-publication-committee-chair@cern.ch

Abstract: A search is performed for events consistent with the pair production of a new heavy particle that acts as a mediator between a dark sector and normal matter, and that decays to a light quark and a new fermion called a dark quark. The search is based on data corresponding to an integrated luminosity of $16.1\,\text{fb}^{-1}$ from proton-proton collisions at $\sqrt{s} = 13\,\text{TeV}$ collected by the CMS experiment at the LHC in 2016. The dark quark is charged only under a new quantum-chromodynamics-like force, and forms an "emerging jet" via a parton shower, containing long-lived dark hadrons that give rise to displaced vertices when decaying to standard model hadrons. The data are consistent with the expectation from standard model processes. Limits are set at 95% confidence level excluding dark pion decay lengths between 5 and 225 mm for dark mediators with masses between 400 and 1250 GeV. Decay lengths smaller than 5 and greater than 225 mm are also excluded in the lower part of this mass range. The dependence of the limit on the dark pion mass is weak for masses between 1 and 10 GeV. This analysis is the first dedicated search for the pair production of a new particle that decays to a jet and an emerging jet.

https://doi.org/10.1007/JHEP02(2019)179

Contents

1 Introduction

Although many astrophysical observations indicate the existence of dark matter [1], it has yet to be observed in the laboratory. While it is possible that dark matter has only gravitational interactions, many compelling models of new physics contain a dark matter candidate that interacts with quarks. One class of models includes new, electrically-neutral fermions called "dark quarks", Q_{DK}, which are not charged under the forces of the standard model (SM) but are charged under a new force in the dark sector ("dark QCD") that has confining properties similar to quantum chromodynamics (SM QCD) [2, 3]. Unlike models based on the popular weakly interacting neutral particle paradigm [4], such models naturally explain the observed mass densities of baryonic matter and dark matter [5].

We consider, in particular, the dark QCD model of Bai, Schwaller, Stolarski, and Weiler (BSSW) that predicts "emerging jets" (EMJ) [6, 7]. Emerging jets contain electrically charged SM particles that are consistent with having been created in the decays of new long-lived neutral particles (dark hadrons), produced in a parton-shower process by dark QCD. In this model, dark QCD has an $\mathrm{SU}(N_{C_{\mathrm{DK}}})$ symmetry, where $N_{C_{\mathrm{DK}}}$ is the number of dark colors. The particle content of the model consists of the dark fermions, the dark gluons associated with the force, and a mediator particle that is charged under both the new dark force and under SM QCD, thus allowing interactions with quarks. The dark fermions are bound by the new force into dark hadrons. These hadrons decay via the mediator to SM hadrons.
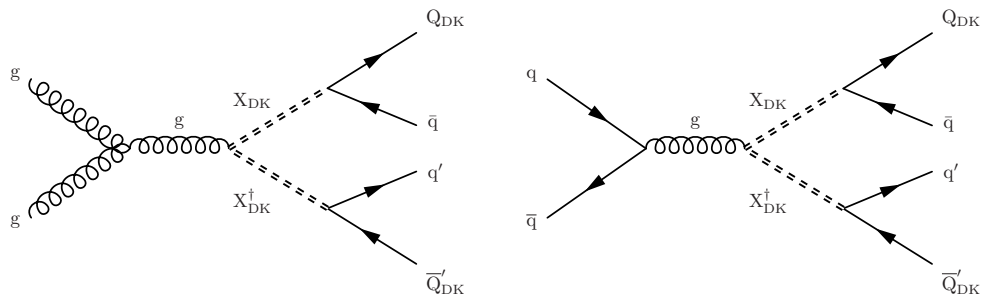
Figure 1. Feynman diagrams in the BSSW model for the pair production of mediator particles, with each mediator decaying to a quark and a dark quark Q_{DK}, via gluon-gluon fusion (left) and quark-antiquark annihilation (right).

The mediator X_{DK} is a complex scalar. Under SM QCD, it is an SU(3) color triplet, and thus can be pair produced via gluon fusion (figure 1, left) or quark-antiquark annihilation (figure 1, right) at the CERN LHC. The mediator has an electric charge of either 1/3 or 2/3 of the electron charge, and it can decay to a right-handed quark with the same charge and a Q_{DK} via Yukawa couplings. There are restrictions on the values of the Yukawa couplings from searches for flavor-changing neutral currents, neutral meson mixing, and rare decays [8–11]. We abide by these restrictions by assuming that all the Yukawa couplings are negligible except for the coupling to the down quark [8–11].

The decay length of the lightest dark meson (dark pion) [7], is given by eq. (1.1):

$$c\tau \approx 80\,\text{mm} \left(\frac{1}{\kappa^4}\right) \left(\frac{2\,\text{GeV}}{f_{\pi_{DK}}}\right)^2 \left(\frac{100\,\text{MeV}}{m_{\text{down}}}\right)^2 \left(\frac{2\,\text{GeV}}{m_{\pi_{DK}}}\right) \left(\frac{m_{X_{DK}}}{1\,\text{TeV}}\right)^4, \tag{1.1}$$

where κ is the appropriate element of the $N_{C_{DK}} \times 3$ matrix of Yukawa couplings between the mediator particle, the quarks, and the dark quarks; $f_{\pi_{DK}}$ is the dark pion decay constant; and m_{down}, $m_{\pi_{DK}}$, and $m_{X_{DK}}$ are the masses of the down quark, the dark pion, and the mediator particle, respectively.

The signature for this search thus consists of four high transverse momentum (p_T) jets, two from down quarks and two from dark quarks. The dark quark jets contain many displaced vertices arising from the decays of the dark pions produced in the dark parton shower and fragmentation. For models with dark hadron decay lengths comparable to the size of the detector, there can also be significant missing transverse momentum (p_T^{miss}). The main background for this signature is SM four-jet production, where jet(s) are tagged as emerging either because they contain long-lived B mesons or because of track misreconstruction, and large artificial p_T^{miss} is created because of jet energy mismeasurement. We use a photon+jets data sample to measure the probability for an SM jet to pass selection criteria designed for emerging jets, and use this probability in estimating the background, as described in section 5.

2 The CMS detector and event reconstruction

The CMS detector is a multipurpose apparatus designed to study physics processes in proton-proton (pp) and heavy ion collisions. A superconducting solenoid occupies its cen-

tral region, providing a magnetic field of 3.8 T parallel to the beam direction. The silicon tracker system consists of 1 440 silicon pixel and 15 148 silicon strip detector modules. The trajectories of charged particles within the pseudorapidity range $|\eta| < 2.5$ are reconstructed from the hits in the silicon tracking system using an iterative procedure with a Kalman filter [12]. The tracking efficiency for prompt hadrons is typically over 98% for tracks with p_T above 1 GeV. For nonisolated particles with $1 < p_T < 10$ GeV and $|\eta| < 1.4$, the track resolutions are typically 1.5% in p_T and 25–90 (45–150) μm in the transverse (longitudinal) impact parameter [12]. The reconstruction efficiency is low for tracks with an impact parameter larger than 25 cm [12].

A lead tungstate crystal electromagnetic calorimeter (ECAL) and a brass/scintillator hadron calorimeter (HCAL) surround the tracking volume and cover $|\eta| < 3$. A steel and quartz-fiber Cherenkov hadron forward calorimeter extends the coverage to $|\eta| < 5$. The muon system consists of gas-ionization detectors embedded in the steel flux return yoke outside the solenoid, and covers $|\eta| < 2.4$. The first level of the CMS trigger system [13] is designed to select events in less than 4 μs, using information from the calorimeters and muon detectors. The high-level trigger (HLT) processor farm then reduces the event rate to around 1 kHz before data storage.

A more detailed description of the CMS detector, together with a definition of the coordinate system and the relevant kinematic variables, can be found in ref. [14].

The pp interaction vertices are reconstructed by clustering tracks on the basis of their z coordinates along the beamline at their points of closest approach to the center of the luminous region using a deterministic annealing algorithm [15]. The position of each vertex is estimated with an adaptive vertex fit [16]. The resolution in the position is around 10–12 μm in each of the three spatial directions [12].

The reconstructed vertex with the largest value of summed physics-object p_T^2 is taken to be the primary pp interaction vertex (PV). The physics objects are the jets, clustered using the jet finding algorithm [17, 18] with the tracks assigned to the vertex as inputs, and the associated p_T^{miss}, taken as the negative vector sum of the p_T of those jets. Other vertices in the same event due to additional pp collisions in the same beam crossing are referred to as pileup.

The particle-flow (PF) algorithm [19] is used to reconstruct and identify each individual particle, with an optimized combination of information from the various elements of the CMS detector. The energy of each photon is directly obtained from the ECAL measurement, corrected for zero-suppression effects. The energy of each electron is determined from a combination of the track momentum at the PV, the corresponding ECAL cluster energy, and the energy sum of all bremsstrahlung photons attached to the track. The energy of each muon is obtained from the corresponding track momentum. The energy of each charged hadron is determined from a combination of the track momentum and the corresponding ECAL and HCAL energies, corrected for zero-suppression effects and for the response functions of the calorimeters to hadronic showers. Finally, the energy of neutral hadrons is obtained from the corresponding corrected ECAL and HCAL energies.

The analysis involves two types of jets: SM QCD jets and emerging jets. For each event, the reconstruction of both types of jets starts with the clustering of reconstructed

particles with the infrared and collinear safe anti-k_T algorithm [17, 18], with a distance parameter R of 0.4. The jet momentum is determined as the vectorial sum of the momenta of associated particles. Additional identification criteria for the emerging jets are given in section 4. For the SM jets, the momentum is found in the simulation to be within 5 to 10% of the true momentum for jets, created from the fragmentation of SM quarks and gluons, over the entire p_T spectrum and detector acceptance. Additional proton-proton interactions within the same or nearby bunch crossings can contribute additional tracks and calorimetric energy depositions to the jet momentum. To mitigate this effect, charged hadrons not associated with the PV are removed from the list of reconstructed particles using the pileup charged-hadron subtraction algorithm [19], while an offset correction is applied to correct for remaining contributions [20–22]. Jet energy corrections are derived from simulation and are confirmed with in situ measurements with the energy balance of Drell-Yan+jet, dijet, multijet, and photon+jet events [23].

Jets consistent with the fragmentation of b quarks are identified using the Combined Secondary Vertex version 2 (CSVv2) discriminator [24]. The loose working point corresponds to correctly identifying a b quark jet with a probability of 81% and misidentifying a light-flavor jet as a b quark jet with a probability of 8.9%.

The $\vec{p}_T^{\,\mathrm{miss}}$ is the negative vector sum of the $\vec{p}_T$ of all PF candidates in an event. Its magnitude is referred to as p_T^{miss}.

3 Simulated samples

Simulated Monte Carlo (MC) samples are used for the estimation of the signal acceptance A, defined as the fraction of MC events passing the selection criteria, and thus including, e.g., tracking and other efficiencies. These samples are also used for the construction of the templates for background estimation and the validation of background estimation techniques. The simulation of SM processes, unless otherwise stated, is performed at leading order in the strong coupling constant using MadGraph5_aMC@NLO 2.2.2 [25] or pythia 8.2 [26] with the NNPDF3.0 [27] parton distribution functions (PDFs). The strong coupling constant at the Z mass scale is set to 0.130 in the generator. Parton shower development and hadronization are simulated with pythia using the underlying-event tune CUETP8M1 [28].

Signal samples are generated with the "hidden valley" model framework in pythia 8.212, using modifications discussed in ref. [7]. The model has several parameters: the mass of the mediator particle, the width of the mediator particle, the number of dark colors, the number of dark flavors, the matrix of Yukawa couplings between the Q_{DK} and the quarks with the same electric charge as the mediator, the dark force confinement scale, the masses of the Q_{DK} (one for each dark flavor), the mass of the dark pion, the dark pion proper decay length, and the mass of the dark rho meson. Following ref. [7], we assume that there are three dark colors and seven dark flavors as suggested in ref. [6]. We assume that all Q_{DK} (and therefore dark pions) are mass degenerate and that the Q_{DK} mass equals the dark force confinement scale. The mass of the dark pion is assumed to be one half the mass of the Q_{DK}. The mass of the dark rho meson is taken to be four times larger than

Signal model parameters	List of values
Dark mediator mass $m_{X_{DK}}$ [GeV]	400, 600, 800, 1000, 1250, 1500, 2000
Dark pion mass $m_{\pi_{DK}}$ [GeV]	1, 2, 5, 10
Dark pion decay length $c\tau_{\pi_{DK}}$ [mm]	1, 2, 5, 25, 45, 60, 100, 150, 225, 300, 500, 1000

Table 1. Parameters used in generating the 336 simulated signal event samples. A sample corresponding to a single model was created for each possible set of parameter values.

the mass of the dark pion. The width of the mediator particle is assumed to be small as compared with the detector mass resolution. These assumptions leave the mediator mass $m_{X_{DK}}$, the dark pion mass $m_{\pi_{DK}}$, and the dark pion proper decay length $c\tau_{\pi_{DK}}$ as free parameters. Samples are generated for all permutations of the values of these parameters listed in table 1. Each set of values defines a single model.

The range in the mediator particle mass over which the search is sensitive depends on the mediator particle pair production cross section. The mediator particle has the same SM quantum numbers as the supersymmetric partner of an SM quark (squark) [7]. Because we assume three dark colors, the signal production cross section is assumed to be three times larger than that for the pair production of a single flavor of squark of the same mass. We use a calculation of the squark pair production cross section that is based on simplified topologies [29–33], with other squarks and gluinos decoupled. The cross section is calculated at next-to-leading order in SM QCD with next-to-leading logarithm soft-gluon resummation [34].

For all samples, multiple minimum-bias events simulated with PYTHIA, with the multiplicity distribution matching that observed in data, are superimposed with the primary interaction event to model the pileup contribution. Generated particles are processed through the full GEANT4-based simulation of the CMS detector [35, 36].

4 Event selection

The analysis is based on data from pp collisions at $\sqrt{s} = 13$ TeV, corresponding to an integrated luminosity of 16.1 fb^{-1} collected by the CMS detector in 2016. The data were obtained using a trigger based on the p_T of the jets in an event. At the HLT, events were selected if they passed a 900 GeV threshold on the scalar p_T sum of all hadronic jets. This analysis used only a portion of the data collected during 2016 because, for part of that running period, saturation-induced dead time was present in the readout of the silicon strip tracker. Such data were not analyzed because of hard-to-model instantaneous luminosity-dependent inefficiencies for the reconstruction of tracks, in particular those tracks with impact parameters larger than 10 mm that are key to the selection of the emerging jet signature.

An emerging jet contains multiple displaced vertices and thus multiple tracks with large impact parameters. Since impact parameter-based variables give good discrimination between SM and emerging jets, we do not attempt to reconstruct the individual decay vertices of the dark pions. Emerging jet candidates are required to have $|\eta| < 2.0$, corre-

sponding to the region of the tracker where the impact parameter resolution is best. Tracks are associated with the candidate if they have $p_T > 1\,\text{GeV}$, pass the "high-purity" quality selection described in ref. [12], and are within a cone of $R = \sqrt{(\Delta\eta)^2 + (\Delta\phi)^2} = 0.4$ (where ϕ is azimuthal angle in radians) around the direction of the jet momentum. Emerging jet candidates are required to have at least one associated track so that the impact parameter can be estimated. The jet candidates are also required to have less than 90% of their energy from electrons and photons, to reduce backgrounds from electrons. Four variables, similar to the ones defined in ref. [37], are used to select the emerging jets. The median of the unsigned transverse impact parameters of associated tracks ($\langle IP_{2D}\rangle$) is correlated with the dark meson proper decay length, and should be small for SM jets and large for emerging jets. The distance between the z position of the track at its distance of closest approach to the PV and the z position of the PV (PU_{dz}) is used to reject tracks from pileup vertices. A variable called D_N, defined as

$$D_N = \sqrt{\left[\frac{z_{PV} - z_{trk}}{0.01\,\text{cm}}\right]^2 + [IP_{sig}]^2}, \tag{4.1}$$

where z_{PV} is the z position of the primary vertex, z_{trk} is the z of the track at its closest approach to the PV, and IP_{sig} is the transverse impact parameter significance of the track at its closest approach to the PV, is used to identify tracks that have an impact parameter that is inconsistent with zero within uncertainties. The variable D_N is smaller for tracks from prompt particles. A variable called α_{3D}, which is the scalar p_T sum of the associated tracks whose values of D_N are smaller than a threshold, divided by the scalar p_T sum of all associated tracks, is used to quantify the fraction of the p_T of the jet that is associated with prompt tracks. This variable should be large for SM jets and small for emerging jets. Figure 2 shows the distributions of $\langle IP_{2D}\rangle$ for background and for signals with a mediator mass of 1 TeV and a dark pion of various masses and with a proper decay length of 25 mm. Figure 3 shows the distributions of α_{3D} for background and for signals with a mediator mass of 1 TeV and a dark pion mass of 5 GeV.

Since the efficacy of the variables used to select emerging jets depends on the correct identification and reconstruction of the PV, additional selections are used to remove rare cases observed in simulated background events where the PV was either not reconstructed or a pileup vertex was chosen as the PV. We require that the chosen PV be the vertex with the largest scalar p_T sum of its associated tracks. We also require that the scalar p_T sum of tracks whose extrapolated separation in z from the PV, at the point of closest approach, is less than 0.01 cm, be larger than 10% of the sum over all tracks.

Selected candidate events are required to have four jets with $|\eta| < 2.0$ and to pass a threshold on the scalar p_T sum of these jets (H_T). They must have either two jets tagged as emerging, or one jet tagged as emerging and large p_T^{miss}. The selection requirements on the jet-p_T thresholds and the emerging jet selection criteria were optimized for each signal model listed in table 1 as follows. For each variable listed in tables 2 and 3, a set of potential selection thresholds were chosen based on the distribution of the variable for signal and background. For each permutation of all the selection thresholds, we calculated the predicted pseudo-significance for each signal model, defined as $S/\sqrt{S + B + (0.1B)^2}$,
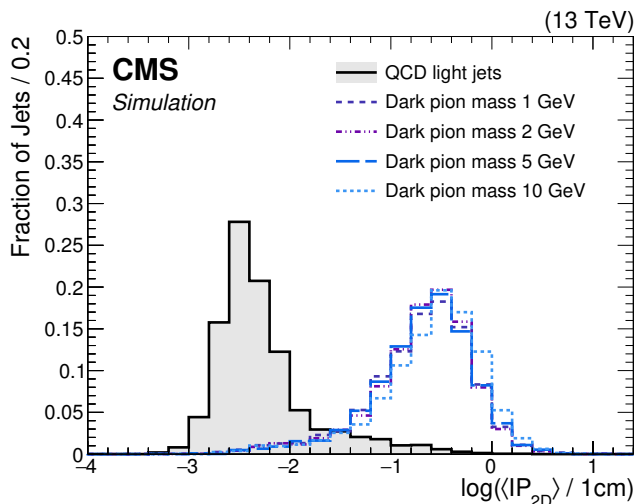
Figure 2. Distributions of $\langle IP_{2D} \rangle$ for background (black) and for signals with a mediator mass of 1 TeV and a dark pion proper decay length of 25 mm, for various dark pion masses.
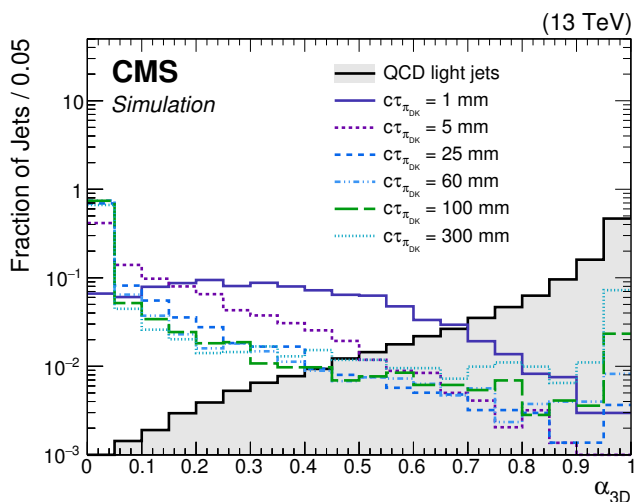

Figure 3. Distributions of α_{3D} for background (black) and for signals with a mediator mass of 1 TeV and a dark pion mass of 5 GeV for dark pion proper decay lengths ranging from 1 to 300 mm.

where S and B correspond to the number of signal and background events and the 0.1 corresponds to an estimate of the systematic uncertainty. In order to limit the final number of background calculations, the pseudo-significances were used to find the minimum number of selection criteria where the difference in pseudo-significance between the best selection thresholds and a chosen selection threshold is no more than 10%, resulting in a total of seven selection sets. In table 2, the selection criteria used to select emerging jets are listed. These jet-level selection criteria, along with event-level kinematic selection criteria, comprise the final selection criteria, given in table 3. There are six groups of criteria used to select emerging jets. The seven selection sets used to define signal regions are given in table 3 (sets 1 to 7), which gives the selections on kinematic variables, along with the corresponding emerging jet criteria from table 2. Two basic categories of selections

Criteria group	PU_dz $(<)$ [cm]	D_N $(<)$	$\langle IP_\mathrm{2D} \rangle$ $(>)$ [cm]	α_3D $(<)$
EMJ-1	2.5	4	0.05	0.25
EMJ-2	4.0	4	0.10	0.25
EMJ-3	4.0	20	0.25	0.25
EMJ-4	2.5	4	0.10	0.25
EMJ-5	2.5	20	0.05	0.25
EMJ-6	2.5	10	0.05	0.25
EMJ-7	2.5	4	0.05	0.40
EMJ-8	4.0	20	0.10	0.50

Table 2. Groups of requirements (associated operator indicated in parentheses) on the variables used in the identification of emerging jets. The groups EMJ-1 to -6 are used for the selection sets that define the signal regions, while the groups EMJ-7 and -8 are used to define SM QCD-enhanced samples for the tests of the background estimation methods.

emerge. Other than set 3, the signal region selection sets require two jets pass emerging jet criteria, and have no requirement on $p_\mathrm{T}^\mathrm{miss}$. Selection set 3 requires that one jet satisfies the emerging jet criteria, and includes a requirement on $p_\mathrm{T}^\mathrm{miss}$. Note that in addition to the $p_\mathrm{T}^\mathrm{miss}$ requirement, the EMJ-3 group imposes the loosest criteria on PU_dz and D_N, and the tightest requirement on $\langle IP_\mathrm{2D} \rangle$, favoring more displaced tracks. Selection set 3 is used for signal models with dark pions with large proper decay lengths. The selection on $\langle IP_\mathrm{2D} \rangle$ is large enough that it removes most events containing b quark jets with tracks with large impact parameters due to the b lifetime; most SM jets thus selected have tracks with large impact parameters due to misreconstruction. The substantive requirement on the $p_\mathrm{T}^\mathrm{miss}$ for this selection set is essential to attain background rejection equivalent to that obtained when requiring two emerging jet candidates.

Since the initial optimization only used a rough estimate of the systematic uncertainty, the final selection set for each model is chosen from among the seven as the one that gives the most stringent expected limit, taking into account more realistic systematic uncertainties.

We also define two additional groups of jet-level criteria that are used to test the effectiveness of the background estimation methods, described in section 5. The EMJ-7 group has the same PU_dz, D_N, and $\langle IP_\mathrm{2D} \rangle$ criteria as EMJ-1 set, but loosens only $\alpha_\mathrm{3D} < 0.4$, while the EMJ-8 group has the same PU_dz and D_N criteria as EMJ-3 set, but loosens $\langle IP_\mathrm{2D} \rangle > 0.10$ and $\alpha_\mathrm{3D} < 0.5$. These two groups of jet-level criteria are more efficient for quark or gluon jets than those used for the final selections in the analysis, improving the statistical power of the tests.

The acceptance of the selection criteria for signal events ranges from a few percent for models with a mediator mass of $400\,\mathrm{GeV}$ to 48% for more massive mediators with a dark pion decay length of $25\,\mathrm{mm}$. Figure 4 shows an example of the signal acceptance of models with dark pion mass of $5\,\mathrm{GeV}$ as a function of the mediator mass and the dark pion proper decay length, with text indicating the corresponding selection set number.

Set number	H_T	$p_{T,1}$	$p_{T,2}$	$p_{T,3}$	$p_{T,4}$	p_T^{miss}	$n_{EMJ}(\geq)$	EMJ group	no. models
1	900	225	100	100	100	0	2	1	12
2	900	225	100	100	100	0	2	2	2
3	900	225	100	100	100	200	1	3	96
4	1100	275	250	150	150	0	2	1	49
5	1000	250	150	100	100	0	2	4	41
6	1000	250	150	100	100	0	2	5	33
7	1200	300	250	200	150	0	2	6	103
8	900	225	100	100	100	0	2	7	SM QCD-enhanced
9	900	225	100	100	100	200	1	8	

Table 3. The seven optimized selection sets used for this search, and the two SM QCD-enhanced selections (sets 8 and 9) used in tests of the background estimation methods. The headers of the columns are: the scalar p_T sum of the four leading jets (H_T) [GeV], the requirements on the p_T of the jets ($p_{T,i}$) [GeV], the requirement on p_T^{miss} [GeV], the minimum number of the four leading jets that pass the emerging jet selection (n_{EMJ}), and the EMJ criteria group described in table 2. The last column is the total number of models defined in table 1 for which the associated selection set gives the best expected sensitivity.
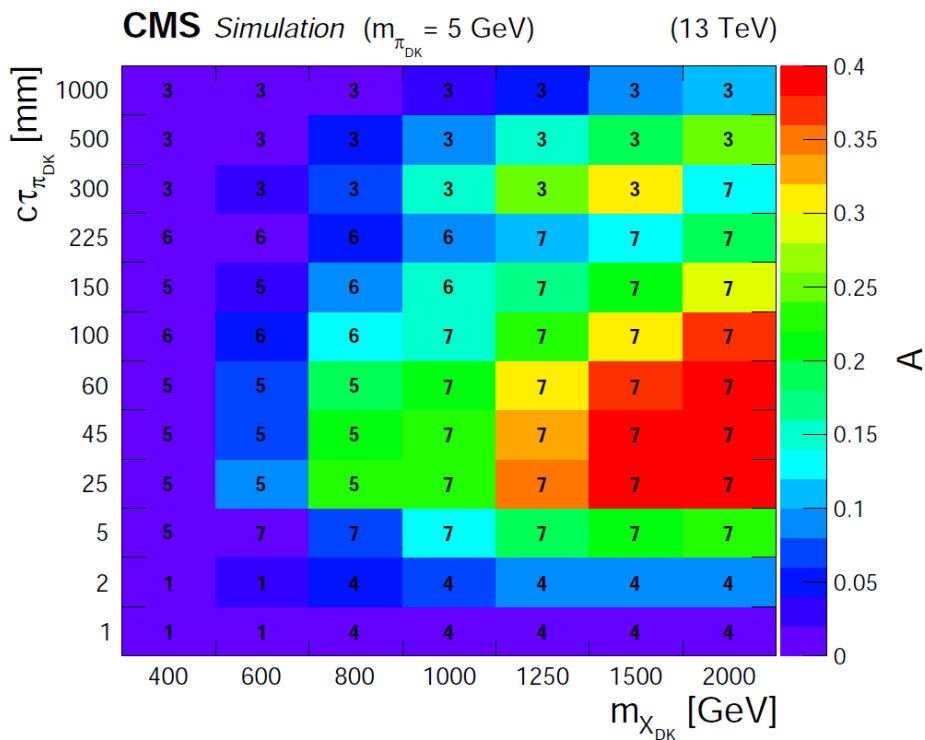

Figure 4. The signal acceptance A, defined as the fraction of simulated signal events passing the selection criteria, for models with a dark pion mass $m_{\pi_{DK}}$ of 5 GeV as a function of the mediator mass $m_{X_{DK}}$ and the dark pion proper decay length $c\tau_{\pi_{DK}}$. The corresponding selection set number for each model is indicated as text on the plot.

5 Background estimation

The production of events containing four SM jets can mimic the signal when two of the jets pass the emerging jet criteria, or when one passes and jet mismeasurement results in artificial p_T^{miss}. The background contributions for each of the selection sets are calculated in two different ways, using the probability for an SM QCD jet to pass the emerging jet requirements.

In the first method, for selection sets 3 and 9 that require at least one emerging jet candidate and p_T^{miss}, the background is calculated using eq. (5.1),

$$N_{bkg,EMJ} = \sum_{events} P_{EMJ}, \tag{5.1}$$

where $N_{bkg,EMJ}$ is the predicted background and P_{EMJ} is the probability for at least one of the four leading p_T jets to pass the emerging jet criteria. The sum is over all events in a "control sample" defined using all the selection requirements for this set except for the requirement of at least one emerging jet candidate. Instead, events are vetoed if one of the four leading p_T jets passes the emerging jet selection. The misidentification probability of each jet is calculated using eq. (5.2).

$$\epsilon_f = \epsilon_{fb} f_b + \epsilon_{fl} (1 - f_b). \tag{5.2}$$

Here ϵ_{fb} is the misidentification probability for b jets, ϵ_{fl} is the misidentification probability for light-flavor jets, and f_b is the probability that the jet is a b jet. The methodology used to estimate ϵ_{fb}, ϵ_{fl}, and f_b is described below. The probability P_{EMJ} is calculated as shown in eq. (5.3).

$$
\begin{aligned}
P_{EMJ} = & \sum_{i\in jets} \epsilon_f \prod_{j\neq i} (1 - \epsilon_f) + \frac{1}{2} \sum_{i,j\in jets} \epsilon_f \epsilon_f \prod_{k\neq i,j} (1 - \epsilon_f) \\
& + \frac{1}{3} \sum_{i,j,k\in jets} \epsilon_f \epsilon_f \epsilon_f \prod_{m\neq i,j,k} (1 - \epsilon_f) + \frac{1}{4} \sum_{i,j,k,m\in jets} \epsilon_f \epsilon_f \epsilon_f \epsilon_f.
\end{aligned} \tag{5.3}
$$

The other selection sets (1 to 8, excluding set 3) require at least two of the four p_T leading jets to pass emerging jet selection requirements. The background is estimated using eq. (5.1) as well, except that the control sample requires exactly one jet to pass the corresponding emerging jet criteria as well as all other selection requirements for the selection set. In this case, P_{EMJ} is the probability for one additional jet to pass the emerging jet requirements, and is calculated using eq. (5.4).

$$
\begin{aligned}
P_{EMJ} = & \frac{1}{2} \sum_{i\in jets\,not\,candidate} \epsilon_f \prod_{j\neq i} (1 - \epsilon_f) + \frac{1}{3} \sum_{i,j\in jets\,not\,candidate} \epsilon_f \epsilon_f \prod_{k\neq i} (1 - \epsilon_f) \\
& + \frac{1}{4} \sum_{i,j,k\in jets\,not\,candidate} \epsilon_f \epsilon_f \epsilon_f.
\end{aligned} \tag{5.4}
$$

In eq. (5.4) the sum is over jets that do not pass the emerging jet selection criteria.

The probability for an SM jet to pass the emerging jet selection criteria (misidentification) depends on the flavor of the jet and on the number of tracks associated with the jet. The probability for a jet initiated by a b quark (b jet) to pass the selection can be a factor of ten larger than that for a jet initiated by any other type of parton (light-flavor jet). For EMJ-3, because of the requirement that $\langle IP_{2D} \rangle$ be large, the misidentification probability for b jets and light-flavor jets is similar. The misidentification probability has a strong dependence on track multiplicity, ranging from a few percent at low track multiplicities, to values several orders of magnitude smaller at the highest multiplicities.

The misidentification probability is measured as a function of track multiplicity using a sample of events collected with a trigger that requires the presence of an isolated photon with $p_T > 165\,\text{GeV}$. We do not expect any signal contamination in this sample. Two subsamples are created: one with an enhanced and one with a suppressed b quark fraction. The sample with an enhanced fraction of b jets is selected by requiring the event to contain at least one additional jet with $p_T > 50\,\text{GeV}$, beyond the one used in the misidentification probability calculation, that has a value for the discriminator of the CSVv2 algorithm greater than 0.8. The sample with suppressed probability of containing a b jet requires an additional jet with $p_T > 50\,\text{GeV}$ with a CSVv2 discriminator value below 0.2. The b quark fraction of each subsample f_b is determined by fitting the observed distribution of the CSVv2 discriminator to the sum of two templates, one created using simulated b jets and the other simulated light-flavor jets. The misidentification probability as a function of the initiating parton type can then be calculated as follows:

$$\begin{pmatrix} \epsilon_{\text{fb}} \\ \epsilon_{\text{fl}} \end{pmatrix} = \begin{pmatrix} \frac{1-f_{\text{b2}}}{f_{\text{b1}}-f_{\text{b2}}} & \frac{-(1-f_{\text{b1}})}{f_{\text{b1}}-f_{\text{b2}}} \\ \frac{-f_{\text{b2}}}{f_{\text{b1}}-f_{\text{b2}}} & \frac{f_{\text{b1}}}{f_{\text{b1}}-f_{\text{b2}}} \end{pmatrix} \begin{pmatrix} \epsilon_{\text{f1}} \\ \epsilon_{\text{f2}} \end{pmatrix}, \tag{5.5}$$

where ϵ_{f1}, f_{b1}, ϵ_{f2}, and f_{b2} represent the respective misidentification probability and b jet fraction in the two samples. Figure 5 shows the measured misidentification probability for EMJ-1 set.

When convolving the misidentification probabilities with the kinematic characteristics and parton composition of the kinematic samples using eqs. (5.3) and (5.4), the parton composition of the kinematic sample is determined by fitting the CSVv2 distribution to b jet and light-flavor jet templates obtained from MC simulation. Figure 6 shows the resulting fit for the kinematic sample of selection set 1. The b quark content, f_b, is determined separately for all events and for events with at least one jet passing the emerging jet criteria. The first is used for predicting the background fraction for selection set 3, which is the only selection set to require only one emerging jet, the second for the other selection sets.

The method for estimating the background was tested by using the same procedure on simulated samples, verifying that the predicted number of selected events was in good agreement with the results obtained when applying the selection criteria to the samples. For example, the average expected number of events obtained by applying the background estimation method to simulated samples (average expected number of events passing the selection in simulated samples) are 207 ± 30 (231 ± 18) and 52.8 ± 9.2 (52.1 ± 6.2) for selection sets 8 and 9, respectively. The background estimation method was also verified
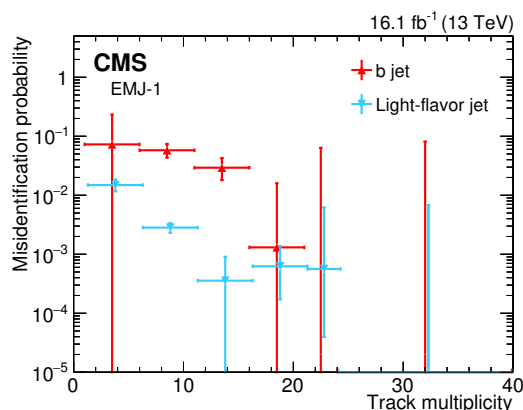
Figure 5. Measured misidentification probability distribution as a function of track multiplicity for the EMJ-1 criteria group defined in table 2. The red up-pointing triangles are for b jets while the blue down-pointing triangles are for light-flavor jets. The horizontal lines on the data points indicate the variable bin width. The uncertainty bars represent the statistical uncertainties of ϵ_{f1}, ϵ_{f2}, f_{b1}, and f_{b2} in eq. (5.5), where the uncertainties in ϵ_{f1} and ϵ_{f2} correspond to Clopper-Pearson intervals [38].

Figure 6. Determination of the b jet fraction by fitting the CSVv2 discriminator distribution. The red and blue distributions are the CSVv2 discriminator templates of b jets and light-flavor jets, respectively. The black points with uncertainty bars show the data distribution. The uncertainties in the upper panel include statistical uncertainties of the b jet and light-flavor jet templates, and the fit uncertainties, summed in quadrature. The goodness of fit is given by the χ^2 divided by the number of degrees of freedom (ndof). The bottom panel shows the difference between data and the fit result, divided by the combination of the statistical uncertainty of data and the uncertainty from the upper panel. The distributions are derived from kinematic samples resulting from selection set 1 in table 3.
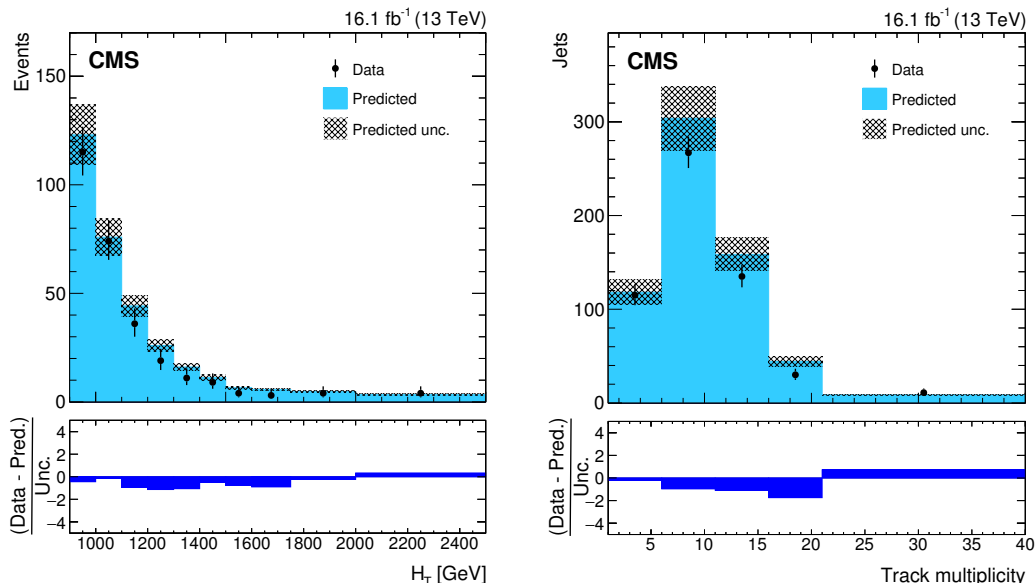
Figure 7. The H_T (left) and number of associated tracks (right) distributions for the observed data events (black points) and the predicted background estimation (blue) for selection set 8 (SM QCD-enhanced), requiring at least two jets tagged by loose emerging jet criteria. The bottom panel shows the difference between observed data and predicted background, divided by the sum in quadrature of the statistical uncertainty in data and the predicted uncertainties from misidentification probability estimation.

using data in the SM QCD-enhanced regions, and the predicted (observed) numbers of events are 317 ± 35 (279) and 115 ± 28 (98), as shown in figures 7 and 8 for selection sets 8 and 9, respectively. The uncertainty in the predicted number combines those due to the number of events in the control sample and statistical uncertainties in the misidentification probabilities.

The background estimation was also tested using a second method for estimating the fraction of b jets in the control samples. The distribution of the measured number of b jets (n_{btag}) per event in a sample is related to the distribution of the true number of b jets per event, the distribution of the true number of non-b jets, the identification probability for b jets, and the misidentification probability for non-b jets. This relationship can be written in the form of a matrix:

$$
\begin{pmatrix} N_{m,0} \\ N_{m,1} \\ N_{m,2} \\ N_{m,3} \\ N_{m,4} \end{pmatrix} = \begin{pmatrix} A_{0,0} & A_{0,1} & A_{0,2} & A_{0,3} & A_{0,4} \\ A_{1,0} & A_{1,1} & A_{1,2} & A_{1,3} & A_{1,4} \\ A_{2,0} & A_{2,1} & A_{2,2} & A_{2,3} & A_{2,4} \\ A_{3,0} & A_{3,1} & A_{3,2} & A_{3,3} & A_{3,4} \\ A_{4,0} & A_{4,1} & A_{4,2} & A_{4,3} & A_{4,4} \end{pmatrix} \begin{pmatrix} N_{t,0} \\ N_{t,1} \\ N_{t,2} \\ N_{t,3} \\ N_{t,4} \end{pmatrix} , \tag{5.6}
$$

where $N_{t,i}$ is the number of events with i b jets and $4 - i$ non-b jets, $N_{m,i}$ is the number of events with i jets passing the CSVv2 loose identification requirements and $4 - i$ failing them, and $A_{i,j}$ is the appropriate combination of the CSVv2 efficiencies for a b jet to pass the identification requirement and for a non-b jet to pass the identification requirement,

including combinatorics. As these probabilities depend on the jet kinematics, the value used is a weighted sum over the jets in the events. This matrix can be inverted to get the number of events as a function of true b jet multiplicity from the number of events as a function of the number of identified b jets. Once the true b jet and non-b jet multiplicities are known, the misidentification probabilities measured from the photon+jets data can be applied.

To build the matrix, first a sample of events passing all the selection requirements of a selection set, except the requirement on the number of emerging jet candidates, is selected. This sample is dominated by SM four-jet production. The number of events with zero, one, two, three, or all of the four leading jets satisfying the CSVv2 loose working point is counted, and the array described in eq. (5.6) is constructed. The array is inverted to obtain the probability $w(\{\nu\}, n_{\mathrm{btag}})$ for each of the $\{\nu\}$ possibilities for the true number of b quarks (0–4). The background is then calculated using eq. (5.7), where each probability is weighted with the appropriate combination of misidentification probabilities, efficiencies, and their combinatorics.

$$N_{\mathrm{bkg,EMJ}}(n_{\mathrm{EMJ}}) = \sum_{\mathrm{events}} \sum_{\nu=0}^{4} P_{\mathrm{EMJ}}(n_{\mathrm{EMJ}}|\{\nu|n_{\mathrm{btag}}\}). \tag{5.7}$$

The probability P_{EMJ} represents the probability of having at least n_{EMJ} jets pass the emerging jet selections given ν true b jets, and is calculated using eq. (5.8).

$$P_{\mathrm{EMJ}}(n_{\mathrm{EMJ}}|\{\nu|n_{\mathrm{btag}}\}) = \sum_{\{n_{\mathrm{EMJ}}|\{\nu\}\}} \frac{w(\{\nu\}, n_{\mathrm{btag}})}{n_{\mathrm{comb}}(\nu)} \prod_{i\in\{n_{\mathrm{EMJ}}\}} p_i \prod_{j\neq i}(1-p_j)$$

$$p_k = p_k(\varphi(\{\nu\})) = \begin{cases} \epsilon_{\mathrm{fb}} \\ \epsilon_{\mathrm{fl}} \end{cases} \tag{5.8}$$

$$n_{\mathrm{comb}}(\nu) = \binom{4}{\nu} = \frac{4!}{\nu!(4-\nu)!}.$$

Here p_k is the flavor-dependent misidentification probability of jet k, and $\varphi(\{\nu\})$ represents all possible flavor assignments of the four jets. The combinatoric factor (n_{comb}) is the binomial coefficient, to account for combinatorics in each permutation in $\{\nu\}$.

The respective numbers of predicted background events for selection sets 8 and 9 are 209.2 ± 1.3 and 53.1 ± 1.2 in simulated samples, and are 312.2 ± 2.0 and 112.0 ± 1.6 for data in SM QCD-enhanced regions. The predicted numbers include only the uncertainty due to the control sample event statistics. The predictions are in good agreement with the primary background estimation method.

6 Systematic uncertainties

The main sources of systematic uncertainty in the background estimate are due to the limited number of events in the photon+jets data and in the simulated samples used for the misidentification probability estimation. Two other sources are the uncertainties in
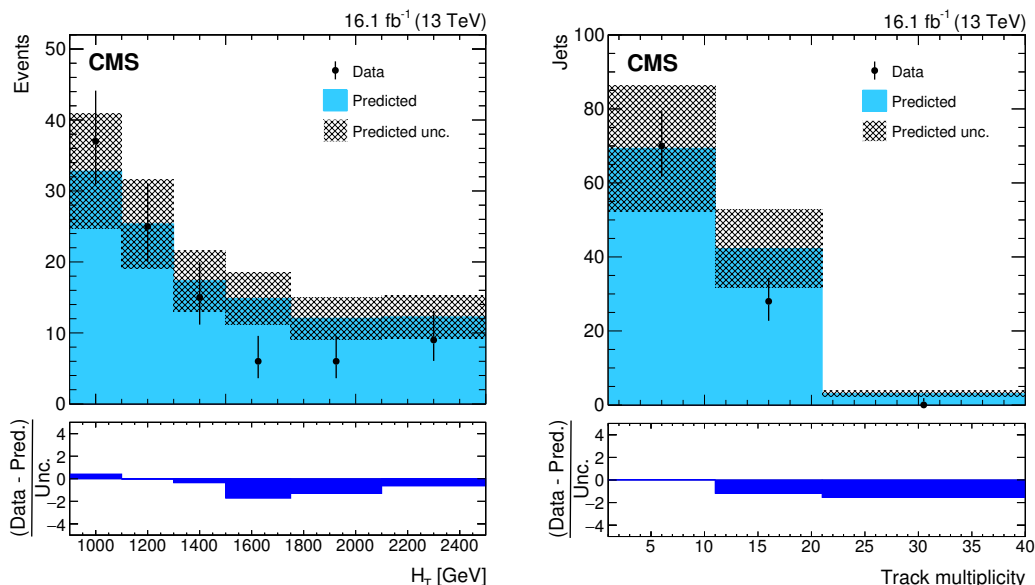
Figure 8. The H_T (left) and number of associated tracks (right) distributions of the observed data events (black points) and the predicted background estimation (blue) for selection set 9 (SM QCD-enhanced), requiring at least one jet tagged by loose emerging jet criteria and large p_T^{miss}. The bottom panel shows the difference between observed data and predicted background, divided by the sum in quadrature of the statistical uncertainty in data and the predicted uncertainties from misidentification probability estimation.

the determination of f_b for each of the samples used in the misidentification probability determination and the uncertainties due to differences in the composition of the non-b jets in the sample used in determining the misidentification probability compared to that in the kinematic samples. We estimate the first uncertainty by using the value of f_b predicted by simulation instead of that obtained by the template fit. We estimate the second uncertainty by using the method on MC simulation. The uncertainty is estimated as the difference in the prediction when using a misidentification probability determined using an MC sample of events containing a high-p_T photon and when using a misidentification probability determined using an MC sample of SM QCD multijet production. The estimated resulting uncertainty for each selection set is given in table 4.

The main source of uncertainty in the estimation of the signal acceptance is the modeling of displaced tracks in the simulation. Other sources include uncertainties in PDFs, MC modeling of the trigger efficiency, integrated luminosity determination, jet energy scale (JES), pileup reweighting, and statistical uncertainties due to the limited size of the MC samples. Systematic uncertainties are largest for the models with the shortest decay lengths.

The uncertainty due to the track modeling in simulation is evaluated by smearing the tracks in signal events using the resolution functions that respectively transform the simulated distributions of $z_{PV} - z_{trk}$ and 2D impact parameter in photon+jet MC samples so that they agree with those in data. The change in signal acceptance when using this transformation is taken as the uncertainty.

Set number	Source of uncertainty (%)	
	b quark fraction	non-b quark composition
1	2.8	1.4
2	0.6	4.4
3	2.9	28.3
4	5.0	4.4
5	0.9	4.0
6	1.6	2.1
7	1.0	6.3

Table 4. Systematic uncertainties affecting the background estimate from control samples in data. For the definition of the selection sets, see table 3.

Source	Uncertainty (%)
Track modeling	<1–3
MC event count	2–17
Integrated luminosity	2.5
Pileup	<1–5
Trigger	6–12
JES	<1–9
PDF	<1–4

Table 5. Ranges of systematic uncertainties over all models given in table 1 for which a 95% CL exclusion is expected, for the uncertainties from different sources.

The acceptance is evaluated using both the MC trigger selection and using a trigger efficiency determined using SM QCD multijet events. The difference is taken as an uncertainty in the acceptance.

The uncertainty in the integrated luminosity determination is 2.5% [39]. The uncertainty due to pileup modeling is measured by varying the total inelastic cross section by 4.6% [40] and reweighting the simulation accordingly. The effect of the JES uncertainty is evaluated by shifting the p_T of jets by the JES uncertainty, and measuring its effect on signal acceptance [23]. The shift in signal acceptance is taken as the uncertainty. We account for variations of the acceptance due to the PDF uncertainties following the PDF4LHC prescription [41]. The resulting ranges of the systematic uncertainties are given in table 5.

7 Results

The number of events passing each selection set, along with the background expectation, is given in table 6. Figure 9 shows a graphical representation of one of the events passing the selection requirements. This event passes both selection set 1 and selection set 5. The display on the left shows the four jets. The display on the right shows the reconstructed tracks in the ρ–ϕ view. The filled circles represent reconstructed secondary vertices, while the grey lines represent the innermost layer of the silicon pixel tracker.

Set number	Expected			Observed	Signal	Model parameters		
						$m_{\mathrm{X_{DK}}}$ [GeV]	$m_{\pi_{\mathrm{DK}}}$ [GeV]	$c\tau_{\pi_{\mathrm{DK}}}$ [mm]
1	$168 \pm$	$15 \pm$	5	131	36.7 ± 4.0	600	5	1
2	$31.8 \pm$	$5.0 \pm$	1.4	47	$(14.6 \pm 2.6) \times 10^2$	400	1	60
3	$19.4 \pm$	$7.0 \pm$	5.5	20	15.6 ± 1.6	1250	1	150
4	$22.5 \pm$	$2.5 \pm$	1.5	16	15.1 ± 2.0	1000	1	2
5	$13.9 \pm$	$1.9 \pm$	0.6	14	35.3 ± 4.0	1000	2	150
6	$9.4 \pm$	$2.0 \pm$	0.3	11	20.7 ± 2.5	1000	10	300
7	$4.40 \pm 0.84 \pm 0.28$			2	5.61 ± 0.64	1250	5	225

Table 6. Expected (mean $\pm$ syst$_1$ $\pm$ syst$_2$) and observed event yields for each selection set. Uncertainties due to the limited number of events in the control sample and statistical uncertainties in the misidentification probabilities are denoted by "syst$_1$", while "syst$_2$" combines the systematic uncertainty sources discussed in table 4. The "Signal" column shows the expected event yield for the heaviest mediator mass that can be excluded for each set, with the systematic uncertainties from sources discussed in table 5 summed in quadrature. The associated model parameters are specified in the last three columns.
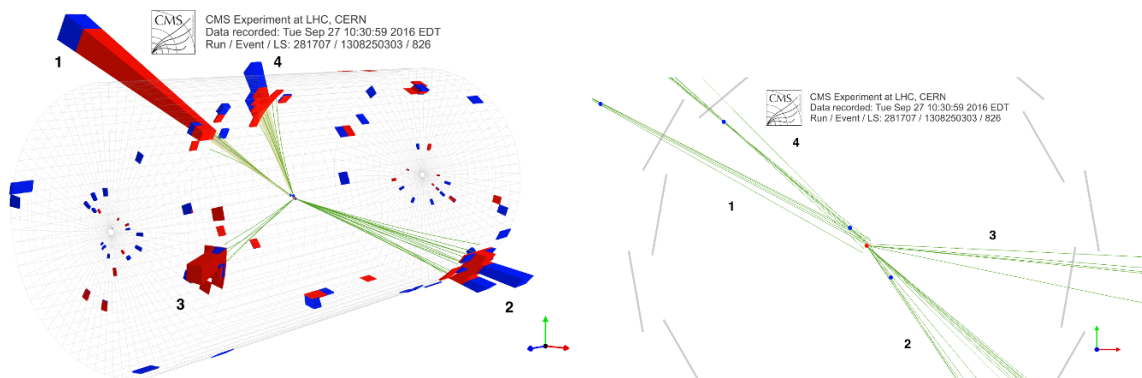

Figure 9. Event display of an event passing both selection set 1 and selection set 5. The event contains four jets (jets 1 and 4 pass the emerging jet criteria), consistent with the decay of two massive mediator particles, each decaying to an SM quark and a dark QCD quark. In such a scenario, the dark mesons produced in the fragmentation of the dark quark would decay back to SM particles via the mediator, resulting in displaced vertices with decay distances on the mm scale. (Left) 3D display: the green lines represent reconstructed tracks, the red (blue) truncated pyramids represent energy in the ECAL (HCAL) detectors, respectively. (Right) Reconstructed tracks in ρ–ϕ view. The filled blue circles represent reconstructed secondary vertices, while the filled red circle is the PV. The solid grey lines represent the innermost layer of the silicon pixel detector.

No significant excess with respect to the SM prediction is observed. A 95% confidence level (CL) cross section upper bound is calculated following the modified frequentist CL$_s$ prescription [42–44], using an asymptotic approximation [45] for the profile likelihood ratio based test statistic, where the systematic uncertainties are taken as nuisance parameters. The 95% CL limits on the signal cross section, expected, and observed exclusion contours on signal parameters are shown in figure 10 for $m_{\pi_{\mathrm{DK}}} = 5$ GeV. The dependence of the limit on $m_{\pi_{\mathrm{DK}}}$ is weak for $m_{\pi_{\mathrm{DK}}}$ between 1 and 10 GeV. Dark pion decay lengths between 5
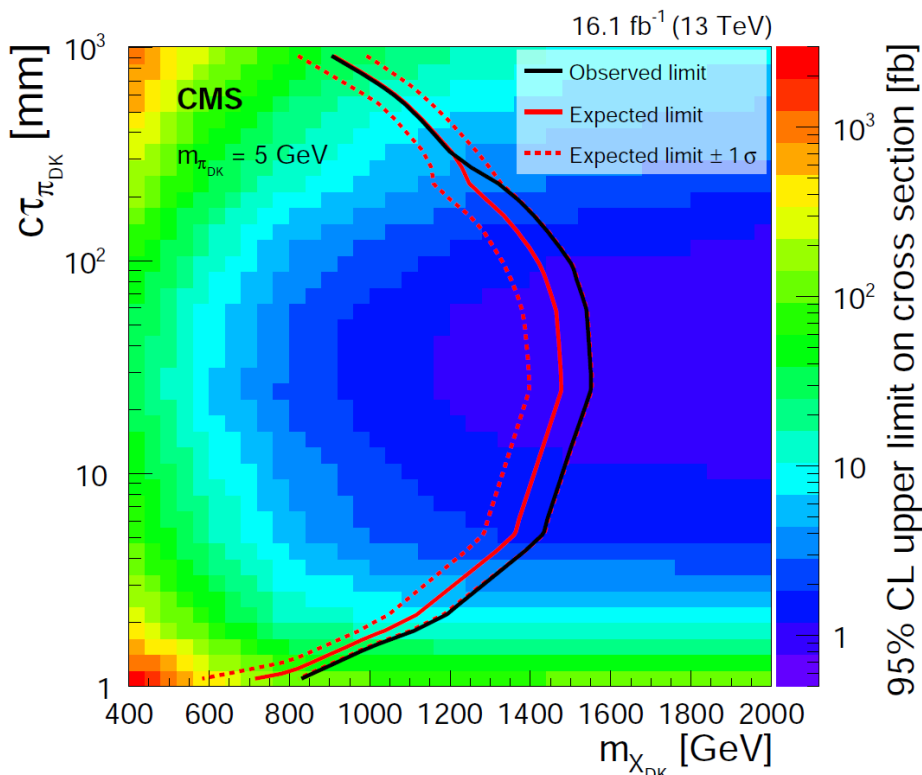
Figure 10. Upper limits at 95% CL on the signal cross section and signal exclusion contours derived from theoretical cross sections for models with dark pion mass $m_{\pi_{DK}}$ of 5 GeV in the $m_{X_{DK}} - c\tau_{\pi_{DK}}$ plane. The solid red contour is the expected upper limit, with its one standard-deviation region enclosed in red dashed lines. The solid black contour is the observed upper limit. The region to the left of the observed contour is excluded.

and 225 mm are excluded at 95% CL for dark mediator masses between 400 and 1250 GeV. Decay lengths smaller than 5 and greater than 225 mm are also excluded in the lower part of this mass range.

8 Summary

A search is presented for events consistent with the pair production of a heavy mediator particle that decays to a light quark and a new fermion called a dark quark, using data from proton-proton collisions at $\sqrt{s} = 13$ TeV corresponding to an integrated luminosity of 16.1 fb^{-1}. The dark quark is assumed to be charged only under a new quantum-chromodynamics-like dark force, and to form an emerging jet via a parton shower, containing long-lived dark hadrons that give rise to displaced vertices when decaying to standard model hadrons. The data are consistent with the expected contributions from standard model processes. Limits are set at 95% confidence level excluding dark pion decay lengths between 5 and 225 mm for dark mediators with masses between 400 and 1250 GeV. Decay lengths smaller than 5 and greater than 225 mm are also excluded in the lower part of this mass range. The dependence of the limit on the dark pion mass is weak for masses between

1 and 10 GeV. This analysis is the first dedicated search for the pair production of a new particle that decays to a jet and an emerging jet.

Acknowledgments

References

[1] B.-L. Young, *A survey of dark matter and related topics in cosmology*, *Front. Phys.* **12** (2017) 121201 [*Erratum ibid.* **12** (2017) 121202] [INSPIRE].

[2] K. Petraki and R.R. Volkas, *Review of asymmetric dark matter*, *Int. J. Mod. Phys.* **A 28** (2013) 1330028 [arXiv:1305.4939] [INSPIRE].

[3] K.M. Zurek, *Asymmetric Dark Matter: Theories, Signatures and Constraints*, *Phys. Rept.* **537** (2014) 91 [arXiv:1308.0338] [INSPIRE].

[4] G. Bertone, D. Hooper and J. Silk, *Particle dark matter: Evidence, candidates and constraints*, *Phys. Rept.* **405** (2005) 279 [hep-ph/0404175] [INSPIRE].

[5] PLANCK collaboration, *Planck 2015 results. XIII. Cosmological parameters*, *Astron. Astrophys.* **594** (2016) A13 [arXiv:1502.01589] [INSPIRE].

[6] Y. Bai and P. Schwaller, *Scale of dark QCD*, *Phys. Rev.* **D 89** (2014) 063522 [arXiv:1306.4676] [INSPIRE].

[7] P. Schwaller, D. Stolarski and A. Weiler, *Emerging Jets*, *JHEP* **05** (2015) 059 [arXiv:1502.05409] [INSPIRE].

[8] J. Brod, J. Drobnak, A.L. Kagan, E. Stamou and J. Zupan, *Stealth QCD-like strong interactions and the $t\bar{t}$ asymmetry*, *Phys. Rev.* **D 91** (2015) 095009 [arXiv:1407.8188] [INSPIRE].

[9] P. Agrawal, M. Blanke and K. Gemmler, *Flavored dark matter beyond Minimal Flavor Violation*, *JHEP* **10** (2014) 072 [arXiv:1405.6709] [INSPIRE].

[10] L. Calibbi, A. Crivellin and B. Zaldívar, *Flavor portal to dark matter*, *Phys. Rev.* **D 92** (2015) 016004 [arXiv:1501.07268] [INSPIRE].

[11] S. Renner and P. Schwaller, *A flavoured dark sector*, *JHEP* **08** (2018) 052 [arXiv:1803.08080] [INSPIRE].

[12] CMS collaboration, *Description and performance of track and primary-vertex reconstruction with the CMS tracker*, 2014 *JINST* **9** P10009 [arXiv:1405.6569] [INSPIRE].

[13] CMS collaboration, *The CMS trigger system*, 2017 *JINST* **12** P01020 [arXiv:1609.02366] [INSPIRE].

[14] CMS collaboration, *The CMS Experiment at the CERN LHC*, 2008 *JINST* **3** S08004 [INSPIRE].

[15] K. Rose, *Deterministic annealing for clustering, compression, classification, regression, and related optimization problems*, *IEEE Proc.* **86** (1998) 2210 [INSPIRE].

[16] R. Frühwirth, W. Waltenberger and P. Vanlaer, *Adaptive vertex fitting*, *J. Phys.* **G 34** (2007) N343 [INSPIRE].

[17] M. Cacciari, G.P. Salam and G. Soyez, *The anti-k_t jet clustering algorithm*, *JHEP* **04** (2008) 063 [arXiv:0802.1189] [INSPIRE].

[18] M. Cacciari, G.P. Salam and G. Soyez, *FastJet User Manual*, *Eur. Phys. J.* **C 72** (2012) 1896 [arXiv:1111.6097] [INSPIRE].

[19] CMS collaboration, *Particle-flow reconstruction and global event description with the CMS detector*, 2017 *JINST* **12** P10003 [arXiv:1706.04965] [INSPIRE].

[20] CMS collaboration, *Determination of Jet Energy Calibration and Transverse Momentum Resolution in CMS*, 2011 *JINST* **6** P11002 [arXiv:1107.4277] [INSPIRE].

[21] M. Cacciari and G.P. Salam, *Pileup subtraction using jet areas*, *Phys. Lett.* **B 659** (2008) 119 [arXiv:0707.1378] [INSPIRE].

[22] CMS collaboration, *Pileup Removal Algorithms*, CMS-PAS-JME-14-001 (2004) [INSPIRE].

[23] CMS collaboration, *Jet energy scale and resolution in the CMS experiment in pp collisions at 8 TeV*, 2017 *JINST* **12** P02014 [arXiv:1607.03663] [INSPIRE].

[24] CMS collaboration, *Identification of heavy-flavour jets with the CMS detector in pp collisions at 13 TeV*, 2018 *JINST* **13** P05011 [arXiv:1712.07158] [INSPIRE].

[25] J. Alwall et al., *The automated computation of tree-level and next-to-leading order differential cross sections and their matching to parton shower simulations*, *JHEP* **07** (2014) 079 [arXiv:1405.0301] [INSPIRE].

[26] T. Sjöstrand et al., *An Introduction to PYTHIA 8.2*, *Comput. Phys. Commun.* **191** (2015) 159 [arXiv:1410.3012] [INSPIRE].

[27] NNPDF collaboration, *Parton distributions for the LHC Run II*, *JHEP* **04** (2015) 040 [arXiv:1410.8849] [INSPIRE].

[28] CMS collaboration, *Event generator tunes obtained from underlying event and multiparton scattering measurements*, *Eur. Phys. J.* **C 76** (2016) 155 [arXiv:1512.00815] [INSPIRE].

[29] N. Arkani-Hamed et al., *MARMOSET: The Path from LHC Data to the New Standard Model via On-Shell Effective Theories*, hep-ph/0703088 [INSPIRE].

[30] J. Alwall, P.C. Schuster and N. Toro, *Simplified Models for a First Characterization of New Physics at the LHC*, *Phys. Rev.* **D 79** (2009) 075020 [arXiv:0810.3921] [INSPIRE].

[31] J. Alwall, M.-P. Le, M. Lisanti and J.G. Wacker, *Model-Independent Jets plus Missing Energy Searches*, *Phys. Rev.* **D 79** (2009) 015005 [arXiv:0809.3264] [INSPIRE].

[32] D.S.M. Alves, E. Izaguirre and J.G. Wacker, *Where the Sidewalk Ends: Jets and Missing Energy Search Strategies for the 7 TeV LHC*, *JHEP* **10** (2011) 012 [arXiv:1102.5338] [INSPIRE].

[33] LHC NEW PHYSICS Working Group, *Simplified Models for LHC New Physics Searches*, *J. Phys.* **G 39** (2012) 105005 [arXiv:1105.2838] [INSPIRE].

[34] C. Borschensky et al., *Squark and gluino production cross sections in pp collisions at $\sqrt{s} = 13$, 14, 33 and 100 TeV*, *Eur. Phys. J.* **C 74** (2014) 3174 [arXiv:1407.5066] [INSPIRE].

[35] GEANT4 collaboration, *GEANT4 — a simulation toolkit*, *Nucl. Instrum. Meth.* **A 506** (2003) 250 [INSPIRE].

[36] GEANT4 collaboration, *Geant4 developments and applications*, *IEEE Trans. Nucl. Sci.* **53** (2006) 270 [INSPIRE].

[37] CMS collaboration, *Search for new long-lived particles at* $\sqrt{s} = 13\,TeV$, *Phys. Lett.* **B 780** (2018) 432 [arXiv:1711.09120] [INSPIRE].

[38] C.J. Clopper and E.S. Pearson, *The use of confidence or fiducial limits illustrated in the case of the binomial*, *Biometrika* **26** (1934) 404.

[39] CMS collaboration, *CMS Luminosity Measurements for the 2016 Data Taking Period*, CMS-PAS-LUM-17-001 (2017) [INSPIRE].

[40] CMS collaboration, *Measurement of the inelastic proton-proton cross section at* $\sqrt{s} = 13\,TeV$, *JHEP* **07** (2018) 161 [arXiv:1802.02613] [INSPIRE].

[41] J. Butterworth et al., *PDF4LHC recommendations for LHC Run II*, *J. Phys.* **G 43** (2016) 023001 [arXiv:1510.03865] [INSPIRE].

[42] T. Junk, *Confidence level computation for combining searches with small statistics*, *Nucl. Instrum. Meth.* **A 434** (1999) 435 [hep-ex/9902006] [INSPIRE].

[43] A.L. Read, *Presentation of search results: The CL_s technique*, *J. Phys.* **G 28** (2002) 2693 [INSPIRE].

[44] ATLAS, CMS collaborations and the LHC Higgs Combination Group, *Procedure for the LHC Higgs boson search combination in Summer 2011*, CMS-NOTE-2011-005 (2011) [ATL-PHYS-PUB-2011-11] [INSPIRE].

[45] G. Cowan, K. Cranmer, E. Gross and O. Vitells, *Asymptotic formulae for likelihood-based tests of new physics*, *Eur. Phys. J.* **C 71** (2011) 1554 [*Erratum ibid.* **C 73** (2013) 2501] [arXiv:1007.1727] [INSPIRE].

The CMS collaboration

Yerevan Physics Institute, Yerevan, Armenia

A.M. Sirunyan, A. Tumasyan

Institut für Hochenergiephysik, Wien, Austria

W. Adam, F. Ambrogi, E. Asilar, T. Bergauer, J. Brandstetter, M. Dragicevic, J. Erö, A. Escalante Del Valle, M. Flechl, R. Frühwirth[1], V.M. Ghete, J. Hrubec, M. Jeitler[1], N. Krammer, I. Krätschmer, D. Liko, T. Madlener, I. Mikulec, N. Rad, H. Rohringer, J. Schieck[1], R. Schöfbeck, M. Spanring, D. Spitzbart, A. Taurok, W. Waltenberger, J. Wittmann, C.-E. Wulz[1], M. Zarucki

Institute for Nuclear Problems, Minsk, Belarus

V. Chekhovsky, V. Mossolov, J. Suarez Gonzalez

Universiteit Antwerpen, Antwerpen, Belgium

E.A. De Wolf, D. Di Croce, X. Janssen, J. Lauwers, M. Pieters, H. Van Haevermaet, P. Van Mechelen, N. Van Remortel

Vrije Universiteit Brussel, Brussel, Belgium

S. Abu Zeid, F. Blekman, J. D'Hondt, J. De Clercq, K. Deroover, G. Flouris, D. Lontkovskyi, S. Lowette, I. Marchesini, S. Moortgat, L. Moreels, Q. Python, K. Skovpen, S. Tavernier, W. Van Doninck, P. Van Mulders, I. Van Parijs

Université Libre de Bruxelles, Bruxelles, Belgium

D. Beghin, B. Bilin, H. Brun, B. Clerbaux, G. De Lentdecker, H. Delannoy, B. Dorney, G. Fasanella, L. Favart, R. Goldouzian, A. Grebenyuk, A.K. Kalsi, T. Lenzi, J. Luetic, N. Postiau, E. Starling, L. Thomas, C. Vander Velde, P. Vanlaer, D. Vannerom, Q. Wang

Ghent University, Ghent, Belgium

T. Cornelis, D. Dobur, A. Fagot, M. Gul, I. Khvastunov[2], D. Poyraz, C. Roskas, D. Trocino, M. Tytgat, W. Verbeke, B. Vermassen, M. Vit, N. Zaganidis

Université Catholique de Louvain, Louvain-la-Neuve, Belgium

H. Bakhshiansohi, O. Bondu, S. Brochet, G. Bruno, C. Caputo, P. David, C. Delaere, M. Delcourt, A. Giammanco, G. Krintiras, V. Lemaitre, A. Magitteri, A. Mertens, K. Piotrzkowski, A. Saggio, M. Vidal Marono, S. Wertz, J. Zobec

Centro Brasileiro de Pesquisas Fisicas, Rio de Janeiro, Brazil

F.L. Alves, G.A. Alves, M. Correa Martins Junior, G. Correia Silva, C. Hensel, A. Moraes, M.E. Pol, P. Rebello Teles

Universidade do Estado do Rio de Janeiro, Rio de Janeiro, Brazil

E. Belchior Batista Das Chagas, W. Carvalho, J. Chinellato[3], E. Coelho, E.M. Da Costa, G.G. Da Silveira[4], D. De Jesus Damiao, C. De Oliveira Martins, S. Fonseca De Souza, H. Malbouisson, D. Matos Figueiredo, M. Melo De Almeida, C. Mora Herrera, L. Mundim, H. Nogima, W.L. Prado Da Silva, L.J. Sanchez Rosas, A. Santoro, A. Sznajder, M. Thiel, E.J. Tonelli Manganote[3], F. Torres Da Silva De Araujo, A. Vilela Pereira

Universidade Estadual Paulista ^{a}, Universidade Federal do ABC ^{b}, São Paulo, Brazil

S. Ahuja^a, C.A. Bernardes^a, L. Calligaris^a, T.R. Fernandez Perez Tomei^a, E.M. Gregores^b, P.G. Mercadante^b, S.F. Novaes^a, SandraS. Padula^a

Institute for Nuclear Research and Nuclear Energy, Bulgarian Academy of Sciences, Sofia, Bulgaria

A. Aleksandrov, R. Hadjiiska, P. Iaydjiev, A. Marinov, M. Misheva, M. Rodozov, M. Shopova, G. Sultanov

University of Sofia, Sofia, Bulgaria

A. Dimitrov, L. Litov, B. Pavlov, P. Petkov

Beihang University, Beijing, China

W. Fang[5], X. Gao[5], L. Yuan

Institute of High Energy Physics, Beijing, China

M. Ahmad, J.G. Bian, G.M. Chen, H.S. Chen, M. Chen, Y. Chen, C.H. Jiang, D. Leggat, H. Liao, Z. Liu, F. Romeo, S.M. Shaheen[6], A. Spiezia, J. Tao, Z. Wang, E. Yazgan, H. Zhang, S. Zhang[6], J. Zhao

State Key Laboratory of Nuclear Physics and Technology, Peking University, Beijing, China

Y. Ban, G. Chen, A. Levin, J. Li, L. Li, Q. Li, Y. Mao, S.J. Qian, D. Wang, Z. Xu

Tsinghua University, Beijing, China

Y. Wang

Universidad de Los Andes, Bogota, Colombia

C. Avila, A. Cabrera, C.A. Carrillo Montoya, L.F. Chaparro Sierra, C. Florez, C.F. González Hernández, M.A. Segura Delgado

University of Split, Faculty of Electrical Engineering, Mechanical Engineering and Naval Architecture, Split, Croatia

B. Courbon, N. Godinovic, D. Lelas, I. Puljak, T. Sculac

University of Split, Faculty of Science, Split, Croatia

Z. Antunovic, M. Kovac

Institute Rudjer Boskovic, Zagreb, Croatia

V. Brigljevic, D. Ferencek, K. Kadija, B. Mesic, A. Starodumov[7], T. Susa

University of Cyprus, Nicosia, Cyprus

M.W. Ather, A. Attikis, M. Kolosova, G. Mavromanolakis, J. Mousa, C. Nicolaou, F. Ptochos, P.A. Razis, H. Rykaczewski

Charles University, Prague, Czech Republic

M. Finger[8], M. Finger Jr.[8]

Escuela Politecnica Nacional, Quito, Ecuador

E. Ayala

Universidad San Francisco de Quito, Quito, Ecuador

E. Carrera Jarrin

Academy of Scientific Research and Technology of the Arab Republic of Egypt, Egyptian Network of High Energy Physics, Cairo, Egypt

Y. Assran[9,10], S. Elgammal[10], S. Khalil[11]

National Institute of Chemical Physics and Biophysics, Tallinn, Estonia

S. Bhowmik, A. Carvalho Antunes De Oliveira, R.K. Dewanjee, K. Ehataht, M. Kadastik, M. Raidal, C. Veelken

Department of Physics, University of Helsinki, Helsinki, Finland

P. Eerola, H. Kirschenmann, J. Pekkanen, M. Voutilainen

Helsinki Institute of Physics, Helsinki, Finland

J. Havukainen, J.K. Heikkilä, T. Järvinen, V. Karimäki, R. Kinnunen, T. Lampén, K. Lassila-Perini, S. Laurila, S. Lehti, T. Lindén, P. Luukka, T. Mäenpää, H. Siikonen, E. Tuominen, J. Tuominiemi

Lappeenranta University of Technology, Lappeenranta, Finland

T. Tuuva

IRFU, CEA, Université Paris-Saclay, Gif-sur-Yvette, France

M. Besancon, F. Couderc, M. Dejardin, D. Denegri, J.L. Faure, F. Ferri, S. Ganjour, A. Givernaud, P. Gras, G. Hamel de Monchenault, P. Jarry, C. Leloup, E. Locci, J. Malcles, G. Negro, J. Rander, A. Rosowsky, M.Ö. Sahin, M. Titov

Laboratoire Leprince-Ringuet, Ecole polytechnique, CNRS/IN2P3, Université Paris-Saclay, Palaiseau, France

A. Abdulsalam[12], C. Amendola, I. Antropov, F. Beaudette, P. Busson, C. Charlot, R. Granier de Cassagnac, I. Kucher, A. Lobanov, J. Martin Blanco, C. Martin Perez, M. Nguyen, C. Ochando, G. Ortona, P. Paganini, P. Pigard, J. Rembser, R. Salerno, J.B. Sauvan, Y. Sirois, A.G. Stahl Leiton, A. Zabi, A. Zghiche

Université de Strasbourg, CNRS, IPHC UMR 7178, Strasbourg, France

J.-L. Agram[13], J. Andrea, D. Bloch, J.-M. Brom, E.C. Chabert, V. Cherepanov, C. Collard, E. Conte[13], J.-C. Fontaine[13], D. Gelé, U. Goerlach, M. Jansová, A.-C. Le Bihan, N. Tonon, P. Van Hove

Centre de Calcul de l'Institut National de Physique Nucleaire et de Physique des Particules, CNRS/IN2P3, Villeurbanne, France

S. Gadrat

Université de Lyon, Université Claude Bernard Lyon 1, CNRS-IN2P3, Institut de Physique Nucléaire de Lyon, Villeurbanne, France

S. Beauceron, C. Bernet, G. Boudoul, N. Chanon, R. Chierici, D. Contardo, P. Depasse, H. El Mamouni, J. Fay, L. Finco, S. Gascon, M. Gouzevitch, G. Grenier, B. Ille, F. Lagarde, I.B. Laktineh, H. Lattaud, M. Lethuillier, L. Mirabito, S. Perries, A. Popov[14], V. Sordini, G. Touquet, M. Vander Donckt, S. Viret

Georgian Technical University, Tbilisi, Georgia

A. Khvedelidze[8]

Tbilisi State University, Tbilisi, Georgia

Z. Tsamalaidze[8]

RWTH Aachen University, I. Physikalisches Institut, Aachen, Germany

C. Autermann, L. Feld, M.K. Kiesel, K. Klein, M. Lipinski, M. Preuten, M.P. Rauch, C. Schomakers, J. Schulz, M. Teroerde, B. Wittmer

RWTH Aachen University, III. Physikalisches Institut A, Aachen, Germany

A. Albert, D. Duchardt, M. Erdmann, S. Erdweg, T. Esch, R. Fischer, S. Ghosh, A. Güth, T. Hebbeker, C. Heidemann, K. Hoepfner, H. Keller, L. Mastrolorenzo, M. Merschmeyer, A. Meyer, P. Millet, S. Mukherjee, T. Pook, M. Radziej, H. Reithler, M. Rieger, A. Schmidt, D. Teyssier, S. Thüer

RWTH Aachen University, III. Physikalisches Institut B, Aachen, Germany

G. Flügge, O. Hlushchenko, T. Kress, A. Künsken, T. Müller, A. Nehrkorn, A. Nowack, C. Pistone, O. Pooth, D. Roy, H. Sert, A. Stahl[15]

Deutsches Elektronen-Synchrotron, Hamburg, Germany

M. Aldaya Martin, T. Arndt, C. Asawatangtrakuldee, I. Babounikau, K. Beernaert, O. Behnke, U. Behrens, A. Bermúdez Martínez, D. Bertsche, A.A. Bin Anuar, K. Borras[16], V. Botta, A. Campbell, P. Connor, C. Contreras-Campana, V. Danilov, A. De Wit, M.M. Defranchis, C. Diez Pardos, D. Domínguez Damiani, G. Eckerlin, T. Eichhorn, A. Elwood, E. Eren, E. Gallo[17], A. Geiser, J.M. Grados Luyando, A. Grohsjean, M. Guthoff, M. Haranko, A. Harb, J. Hauk, H. Jung, M. Kasemann, J. Keaveney, C. Kleinwort, J. Knolle, D. Krücker, W. Lange, A. Lelek, T. Lenz, J. Leonard, K. Lipka, W. Lohmann[18], R. Mankel, I.-A. Melzer-Pellmann, A.B. Meyer, M. Meyer, M. Missiroli, G. Mittag, J. Mnich, V. Myronenko, S.K. Pflitsch, D. Pitzl, A. Raspereza, M. Savitskyi, P. Saxena, P. Schütze, C. Schwanenberger, R. Shevchenko, A. Singh, H. Tholen, O. Turkot, A. Vagnerini, G.P. Van Onsem, R. Walsh, Y. Wen, K. Wichmann, C. Wissing, O. Zenaiev

University of Hamburg, Hamburg, Germany

R. Aggleton, S. Bein, L. Benato, A. Benecke, V. Blobel, T. Dreyer, A. Ebrahimi, E. Garutti, D. Gonzalez, P. Gunnellini, J. Haller, A. Hinzmann, A. Karavdina, G. Kasieczka, R. Klanner, R. Kogler, N. Kovalchuk, S. Kurz, V. Kutzner, J. Lange, D. Marconi, J. Multhaup, M. Niedziela, C.E.N. Niemeyer, D. Nowatschin, A. Perieanu, A. Reimers, O. Rieger, C. Scharf, P. Schleper, S. Schumann, J. Schwandt, J. Sonneveld, H. Stadie, G. Steinbrück, F.M. Stober, M. Stöver, A. Vanhoefer, B. Vormwald, I. Zoi

Karlsruher Institut fuer Technologie, Karlsruhe, Germany

M. Akbiyik, C. Barth, M. Baselga, S. Baur, E. Butz, R. Caspart, T. Chwalek, F. Colombo, W. De Boer, A. Dierlamm, K. El Morabit, N. Faltermann, B. Freund, M. Giffels, M.A. Harrendorf, F. Hartmann[15], S.M. Heindl, U. Husemann, I. Katkov[14], S. Kudella, S. Mitra, M.U. Mozer, Th. Müller, M. Musich, M. Plagge, G. Quast, K. Rabbertz, M. Schröder, I. Shvetsov, H.J. Simonis, R. Ulrich, S. Wayand, M. Weber, T. Weiler, C. Wöhrmann, R. Wolf

Institute of Nuclear and Particle Physics (INPP), NCSR Demokritos, Aghia Paraskevi, Greece

G. Anagnostou, G. Daskalakis, T. Geralis, A. Kyriakis, D. Loukas, G. Paspalaki, I. Topsis-Giotis

National and Kapodistrian University of Athens, Athens, Greece

G. Karathanasis, S. Kesisoglou, P. Kontaxakis, A. Panagiotou, I. Papavergou, N. Saoulidou, E. Tziaferi, K. Vellidis

National Technical University of Athens, Athens, Greece

K. Kousouris, I. Papakrivopoulos, G. Tsipolitis

University of Ioánnina, Ioánnina, Greece

I. Evangelou, C. Foudas, P. Gianneios, P. Katsoulis, P. Kokkas, S. Mallios, N. Manthos, I. Papadopoulos, E. Paradas, J. Strologas, F.A. Triantis, D. Tsitsonis

MTA-ELTE Lendület CMS Particle and Nuclear Physics Group, Eötvös Loránd University, Budapest, Hungary

M. Bartók[19], M. Csanad, N. Filipovic, P. Major, M.I. Nagy, G. Pasztor, O. Surányi, G.I. Veres

Wigner Research Centre for Physics, Budapest, Hungary

G. Bencze, C. Hajdu, D. Horvath[20], Á. Hunyadi, F. Sikler, T.Á. Vámi, V. Veszpremi, G. Vesztergombi[†]

Institute of Nuclear Research ATOMKI, Debrecen, Hungary

N. Beni, S. Czellar, J. Karancsi[21], A. Makovec, J. Molnar, Z. Szillasi

Institute of Physics, University of Debrecen, Debrecen, Hungary

P. Raics, Z.L. Trocsanyi, B. Ujvari

Indian Institute of Science (IISc), Bangalore, India

S. Choudhury, J.R. Komaragiri, P.C. Tiwari

National Institute of Science Education and Research, HBNI, Bhubaneswar, India

S. Bahinipati[22], C. Kar, P. Mal, K. Mandal, A. Nayak[23], D.K. Sahoo[22], S.K. Swain

Panjab University, Chandigarh, India
S. Bansal, S.B. Beri, V. Bhatnagar, S. Chauhan, R. Chawla, N. Dhingra, R. Gupta, A. Kaur, M. Kaur, S. Kaur, P. Kumari, M. Lohan, A. Mehta, K. Sandeep, S. Sharma, J.B. Singh, A.K. Virdi, G. Walia

University of Delhi, Delhi, India
A. Bhardwaj, B.C. Choudhary, R.B. Garg, M. Gola, S. Keshri, Ashok Kumar, S. Malhotra, M. Naimuddin, P. Priyanka, K. Ranjan, Aashaq Shah, R. Sharma

Saha Institute of Nuclear Physics, HBNI, Kolkata, India
R. Bhardwaj[24], M. Bharti[24], R. Bhattacharya, S. Bhattacharya, U. Bhawandeep[24], D. Bhowmik, S. Dey, S. Dutt[24], S. Dutta, S. Ghosh, K. Mondal, S. Nandan, A. Purohit, P.K. Rout, A. Roy, S. Roy Chowdhury, G. Saha, S. Sarkar, M. Sharan, B. Singh[24], S. Thakur[24]

Indian Institute of Technology Madras, Madras, India
P.K. Behera

Bhabha Atomic Research Centre, Mumbai, India
R. Chudasama, D. Dutta, V. Jha, V. Kumar, P.K. Netrakanti, L.M. Pant, P. Shukla

Tata Institute of Fundamental Research-A, Mumbai, India
T. Aziz, M.A. Bhat, S. Dugad, G.B. Mohanty, N. Sur, B. Sutar, RavindraKumar Verma

Tata Institute of Fundamental Research-B, Mumbai, India
S. Banerjee, S. Bhattacharya, S. Chatterjee, P. Das, M. Guchait, Sa. Jain, S. Karmakar, S. Kumar, M. Maity[25], G. Majumder, K. Mazumdar, N. Sahoo, T. Sarkar[25]

Indian Institute of Science Education and Research (IISER), Pune, India
S. Chauhan, S. Dube, V. Hegde, A. Kapoor, K. Kothekar, S. Pandey, A. Rane, S. Sharma

Institute for Research in Fundamental Sciences (IPM), Tehran, Iran
S. Chenarani[26], E. Eskandari Tadavani, S.M. Etesami[26], M. Khakzad, M. Mohammadi Najafabadi, M. Naseri, F. Rezaei Hosseinabadi, B. Safarzadeh[27], M. Zeinali

University College Dublin, Dublin, Ireland
M. Felcini, M. Grunewald

INFN Sezione di Bari [a], **Università di Bari** [b], **Politecnico di Bari** [c], **Bari, Italy**
M. Abbrescia[a,b], C. Calabria[a,b], A. Colaleo[a], D. Creanza[a,c], L. Cristella[a,b], N. De Filippis[a,c], M. De Palma[a,b], A. Di Florio[a,b], F. Errico[a,b], L. Fiore[a], A. Gelmi[a,b], G. Iaselli[a,c], M. Ince[a,b], S. Lezki[a,b], G. Maggi[a,c], M. Maggi[a], G. Miniello[a,b], S. My[a,b], S. Nuzzo[a,b], A. Pompili[a,b], G. Pugliese[a,c], R. Radogna[a], A. Ranieri[a], G. Selvaggi[a,b], A. Sharma[a], L. Silvestris[a], R. Venditti[a], P. Verwilligen[a], G. Zito[a]

INFN Sezione di Bologna [a], **Università di Bologna** [b], **Bologna, Italy**
G. Abbiendi[a], C. Battilana[a,b], D. Bonacorsi[a,b], L. Borgonovi[a,b], S. Braibant-Giacomelli[a,b], R. Campanini[a,b], P. Capiluppi[a,b], A. Castro[a,b], F.R. Cavallo[a], S.S. Chhibra[a,b], C. Ciocca[a], G. Codispoti[a,b], M. Cuffiani[a,b], G.M. Dallavalle[a], F. Fabbri[a], A. Fanfani[a,b], E. Fontanesi,

P. Giacomelli^a, C. Grandi^a, L. Guiducci^{a,b}, F. Iemmi^{a,b}, S. Lo Meo^a, S. Marcellini^a, G. Masetti^a, A. Montanari^a, F.L. Navarria^{a,b}, A. Perrotta^a, F. Primavera^{a,b,15}, T. Rovelli^{a,b}, G.P. Siroli^{a,b}, N. Tosi^a

INFN Sezione di Catania ^{a}, Università di Catania ^{b}, Catania, Italy

S. Albergo^{a,b}, A. Di Mattia^a, R. Potenza^{a,b}, A. Tricomi^{a,b}, C. Tuve^{a,b}

INFN Sezione di Firenze ^{a}, Università di Firenze ^{b}, Firenze, Italy

G. Barbagli^a, K. Chatterjee^{a,b}, V. Ciulli^{a,b}, C. Civinini^a, R. D'Alessandro^{a,b}, E. Focardi^{a,b}, G. Latino, P. Lenzi^{a,b}, M. Meschini^a, S. Paoletti^a, L. Russo^{a,28}, G. Sguazzoni^a, D. Strom^a, L. Viliani^a

INFN Laboratori Nazionali di Frascati, Frascati, Italy

L. Benussi, S. Bianco, F. Fabbri, D. Piccolo

INFN Sezione di Genova ^{a}, Università di Genova ^{b}, Genova, Italy

F. Ferro^a, R. Mulargia^{a,b}, F. Ravera^{a,b}, E. Robutti^a, S. Tosi^{a,b}

INFN Sezione di Milano-Bicocca ^{a}, Università di Milano-Bicocca ^{b}, Milano, Italy

A. Benaglia^a, A. Beschi^b, F. Brivio^{a,b}, V. Ciriolo^{a,b,15}, S. Di Guida^{a,d,15}, M.E. Dinardo^{a,b}, S. Fiorendi^{a,b}, S. Gennai^a, A. Ghezzi^{a,b}, P. Govoni^{a,b}, M. Malberti^{a,b}, S. Malvezzi^a, A. Massironi^{a,b}, D. Menasce^a, F. Monti, L. Moroni^a, M. Paganoni^{a,b}, D. Pedrini^a, S. Ragazzi^{a,b}, T. Tabarelli de Fatis^{a,b}, D. Zuolo^{a,b}

INFN Sezione di Napoli ^{a}, Università di Napoli 'Federico II' ^{b}, Napoli, Italy, Università della Basilicata ^{c}, Potenza, Italy, Università G. Marconi ^{d}, Roma, Italy

S. Buontempo^a, N. Cavallo^{a,c}, A. De Iorio^{a,b}, A. Di Crescenzo^{a,b}, F. Fabozzi^{a,c}, F. Fienga^a, G. Galati^a, A.O.M. Iorio^{a,b}, W.A. Khan^a, L. Lista^a, S. Meola^{a,d,15}, P. Paolucci^{a,15}, C. Sciacca^{a,b}, E. Voevodina^{a,b}

INFN Sezione di Padova ^{a}, Università di Padova ^{b}, Padova, Italy, Università di Trento ^{c}, Trento, Italy

P. Azzi^a, N. Bacchetta^a, D. Bisello^{a,b}, A. Boletti^{a,b}, A. Bragagnolo, R. Carlin^{a,b}, P. Checchia^a, P. De Castro Manzano^a, T. Dorigo^a, U. Dosselli^a, F. Gasparini^{a,b}, U. Gasparini^{a,b}, A. Gozzelino^a, S.Y. Hoh, S. Lacaprara^a, P. Lujan, M. Margoni^{a,b}, A.T. Meneguzzo^{a,b}, J. Pazzini^{a,b}, N. Pozzobon^{a,b}, P. Ronchese^{a,b}, R. Rossin^{a,b}, F. Simonetto^{a,b}, A. Tiko, E. Torassa^a, M. Tosi^{a,b}, M. Zanetti^{a,b}, P. Zotto^{a,b}, G. Zumerle^{a,b}

INFN Sezione di Pavia ^{a}, Università di Pavia ^{b}, Pavia, Italy

A. Braghieri^a, A. Magnani^a, P. Montagna^{a,b}, S.P. Ratti^{a,b}, V. Re^a, M. Ressegotti^{a,b}, C. Riccardi^{a,b}, P. Salvini^a, I. Vai^{a,b}, P. Vitulo^{a,b}

INFN Sezione di Perugia ^{a}, Università di Perugia ^{b}, Perugia, Italy

M. Biasini^{a,b}, G.M. Bilei^a, C. Cecchi^{a,b}, D. Ciangottini^{a,b}, L. Fanò^{a,b}, P. Lariccia^{a,b}, R. Leonardi^{a,b}, E. Manoni^a, G. Mantovani^{a,b}, V. Mariani^{a,b}, M. Menichelli^a, A. Rossi^{a,b}, A. Santocchia^{a,b}, D. Spiga^a

INFN Sezione di Pisa ^{a}, Università di Pisa ^{b}, Scuola Normale Superiore di Pisa ^{c}, Pisa, Italy

K. Androsov^a, P. Azzurri^a, G. Bagliesi^a, L. Bianchini^a, T. Boccali^a, L. Borrello, R. Castaldi^a, M.A. Ciocci^{a,b}, R. Dell'Orso^a, G. Fedi^a, F. Fiori^{a,c}, L. Giannini^{a,c}, A. Giassi^a, M.T. Grippo^a, F. Ligabue^{a,c}, E. Manca^{a,c}, G. Mandorli^{a,c}, A. Messineo^{a,b}, F. Palla^a, A. Rizzi^{a,b}, G. Rolandi[29], P. Spagnolo^a, R. Tenchini^a, G. Tonelli^{a,b}, A. Venturi^a, P.G. Verdini^a

INFN Sezione di Roma ^{a}, Sapienza Università di Roma ^{b}, Rome, Italy

L. Barone^{a,b}, F. Cavallari^a, M. Cipriani^{a,b}, D. Del Re^{a,b}, E. Di Marco^{a,b}, M. Diemoz^a, S. Gelli^{a,b}, E. Longo^{a,b}, B. Marzocchi^{a,b}, P. Meridiani^a, G. Organtini^{a,b}, F. Pandolfi^a, R. Paramatti^{a,b}, F. Preiato^{a,b}, S. Rahatlou^{a,b}, C. Rovelli^a, F. Santanastasio^{a,b}

INFN Sezione di Torino ^{a}, Università di Torino ^{b}, Torino, Italy, Università del Piemonte Orientale ^{c}, Novara, Italy

N. Amapane^{a,b}, R. Arcidiacono^{a,c}, S. Argiro^{a,b}, M. Arneodo^{a,c}, N. Bartosik^a, R. Bellan^{a,b}, C. Biino^a, N. Cartiglia^a, F. Cenna^{a,b}, S. Cometti^a, M. Costa^{a,b}, R. Covarelli^{a,b}, N. Demaria^a, B. Kiani^{a,b}, C. Mariotti^a, S. Maselli^a, E. Migliore^{a,b}, V. Monaco^{a,b}, E. Monteil^{a,b}, M. Monteno^a, M.M. Obertino^{a,b}, L. Pacher^{a,b}, N. Pastrone^a, M. Pelliccioni^a, G.L. Pinna Angioni^{a,b}, A. Romero^{a,b}, M. Ruspa^{a,c}, R. Sacchi^{a,b}, K. Shchelina^{a,b}, V. Sola^a, A. Solano^{a,b}, D. Soldi^{a,b}, A. Staiano^a

INFN Sezione di Trieste ^{a}, Università di Trieste ^{b}, Trieste, Italy

S. Belforte^a, V. Candelise^{a,b}, M. Casarsa^a, F. Cossutti^a, A. Da Rold^{a,b}, G. Della Ricca^{a,b}, F. Vazzoler^{a,b}, A. Zanetti^a

Kyungpook National University, Daegu, Korea

D.H. Kim, G.N. Kim, M.S. Kim, J. Lee, S. Lee, S.W. Lee, C.S. Moon, Y.D. Oh, S.I. Pak, S. Sekmen, D.C. Son, Y.C. Yang

Chonnam National University, Institute for Universe and Elementary Particles, Kwangju, Korea

H. Kim, D.H. Moon, G. Oh

Hanyang University, Seoul, Korea

B. Francois, J. Goh[30], T.J. Kim

Korea University, Seoul, Korea

S. Cho, S. Choi, Y. Go, D. Gyun, S. Ha, B. Hong, Y. Jo, K. Lee, K.S. Lee, S. Lee, J. Lim, S.K. Park, Y. Roh

Sejong University, Seoul, Korea

H.S. Kim

Seoul National University, Seoul, Korea

J. Almond, J. Kim, J.S. Kim, H. Lee, K. Lee, K. Nam, S.B. Oh, B.C. Radburn-Smith, S.h. Seo, U.K. Yang, H.D. Yoo, G.B. Yu

University of Seoul, Seoul, Korea

D. Jeon, H. Kim, J.H. Kim, J.S.H. Lee, I.C. Park

Sungkyunkwan University, Suwon, Korea

Y. Choi, C. Hwang, J. Lee, I. Yu

Vilnius University, Vilnius, Lithuania

V. Dudenas, A. Juodagalvis, J. Vaitkus

National Centre for Particle Physics, Universiti Malaya, Kuala Lumpur, Malaysia

I. Ahmed, Z.A. Ibrahim, M.A.B. Md Ali[31], F. Mohamad Idris[32], W.A.T. Wan Abdullah, M.N. Yusli, Z. Zolkapli

Universidad de Sonora (UNISON), Hermosillo, Mexico

J.F. Benitez, A. Castaneda Hernandez, J.A. Murillo Quijada

Centro de Investigacion y de Estudios Avanzados del IPN, Mexico City, Mexico

H. Castilla-Valdez, E. De La Cruz-Burelo, M.C. Duran-Osuna, I. Heredia-De La Cruz[33], R. Lopez-Fernandez, J. Mejia Guisao, R.I. Rabadan-Trejo, M. Ramirez-Garcia, G. Ramirez-Sanchez, R. Reyes-Almanza, A. Sanchez-Hernandez

Universidad Iberoamericana, Mexico City, Mexico

S. Carrillo Moreno, C. Oropeza Barrera, F. Vazquez Valencia

Benemerita Universidad Autonoma de Puebla, Puebla, Mexico

J. Eysermans, I. Pedraza, H.A. Salazar Ibarguen, C. Uribe Estrada

Universidad Autónoma de San Luis Potosí, San Luis Potosí, Mexico

A. Morelos Pineda

University of Auckland, Auckland, New Zealand

D. Krofcheck

University of Canterbury, Christchurch, New Zealand

S. Bheesette, P.H. Butler

National Centre for Physics, Quaid-I-Azam University, Islamabad, Pakistan

A. Ahmad, M. Ahmad, M.I. Asghar, Q. Hassan, H.R. Hoorani, A. Saddique, M.A. Shah, M. Shoaib, M. Waqas

National Centre for Nuclear Research, Swierk, Poland

H. Bialkowska, M. Bluj, B. Boimska, T. Frueboes, M. Górski, M. Kazana, M. Szleper, P. Traczyk, P. Zalewski

Institute of Experimental Physics, Faculty of Physics, University of Warsaw, Warsaw, Poland

K. Bunkowski, A. Byszuk[34], K. Doroba, A. Kalinowski, M. Konecki, J. Krolikowski, M. Misiura, M. Olszewski, A. Pyskir, M. Walczak

Laboratório de Instrumentação e Física Experimental de Partículas, Lisboa, Portugal

M. Araujo, P. Bargassa, C. Beirão Da Cruz E Silva, A. Di Francesco, P. Faccioli, B. Galinhas, M. Gallinaro, J. Hollar, N. Leonardo, J. Seixas, G. Strong, O. Toldaiev, J. Varela

Joint Institute for Nuclear Research, Dubna, Russia

S. Afanasiev, P. Bunin, M. Gavrilenko, I. Golutvin, I. Gorbunov, A. Kamenev, V. Karjavine, A. Lanev, A. Malakhov, V. Matveev[35,36], P. Moisenz, V. Palichik, V. Perelygin, S. Shmatov, S. Shulha, N. Skatchkov, V. Smirnov, N. Voytishin, A. Zarubin

Petersburg Nuclear Physics Institute, Gatchina (St. Petersburg), Russia

V. Golovtsov, Y. Ivanov, V. Kim[37], E. Kuznetsova[38], P. Levchenko, V. Murzin, V. Oreshkin, I. Smirnov, D. Sosnov, V. Sulimov, L. Uvarov, S. Vavilov, A. Vorobyev

Institute for Nuclear Research, Moscow, Russia

Yu. Andreev, A. Dermenev, S. Gninenko, N. Golubev, A. Karneyeu, M. Kirsanov, N. Krasnikov, A. Pashenkov, D. Tlisov, A. Toropin

Institute for Theoretical and Experimental Physics, Moscow, Russia

V. Epshteyn, V. Gavrilov, N. Lychkovskaya, V. Popov, I. Pozdnyakov, G. Safronov, A. Spiridonov, A. Stepennov, V. Stolin, M. Toms, E. Vlasov, A. Zhokin

Moscow Institute of Physics and Technology, Moscow, Russia

T. Aushev

National Research Nuclear University 'Moscow Engineering Physics Institute' (MEPhI), Moscow, Russia

M. Chadeeva[39], P. Parygin, D. Philippov, S. Polikarpov[39], E. Popova, V. Rusinov

P.N. Lebedev Physical Institute, Moscow, Russia

V. Andreev, M. Azarkin, I. Dremin[36], M. Kirakosyan, S.V. Rusakov, A. Terkulov

Skobeltsyn Institute of Nuclear Physics, Lomonosov Moscow State University, Moscow, Russia

A. Baskakov, A. Belyaev, E. Boos, M. Dubinin[40], L. Dudko, A. Ershov, A. Gribushin, V. Klyukhin, O. Kodolova, I. Lokhtin, I. Miagkov, S. Obraztsov, S. Petrushanko, V. Savrin, A. Snigirev

Novosibirsk State University (NSU), Novosibirsk, Russia

A. Barnyakov[41], V. Blinov[41], T. Dimova[41], L. Kardapoltsev[41], Y. Skovpen[41]

Institute for High Energy Physics of National Research Centre 'Kurchatov Institute', Protvino, Russia

I. Azhgirey, I. Bayshev, S. Bitioukov, D. Elumakhov, A. Godizov, V. Kachanov, A. Kalinin, D. Konstantinov, P. Mandrik, V. Petrov, R. Ryutin, S. Slabospitskii, A. Sobol, S. Troshin, N. Tyurin, A. Uzunian, A. Volkov

National Research Tomsk Polytechnic University, Tomsk, Russia

A. Babaev, S. Baidali, V. Okhotnikov

University of Belgrade, Faculty of Physics and Vinca Institute of Nuclear Sciences, Belgrade, Serbia

P. Adzic[42], P. Cirkovic, D. Devetak, M. Dordevic, J. Milosevic

Centro de Investigaciones Energéticas Medioambientales y Tecnológicas (CIEMAT), Madrid, Spain

J. Alcaraz Maestre, A. Álvarez Fernández, I. Bachiller, M. Barrio Luna, J.A. Brochero Cifuentes, M. Cerrada, N. Colino, B. De La Cruz, A. Delgado Peris, C. Fernandez Bedoya, J.P. Fernández Ramos, J. Flix, M.C. Fouz, O. Gonzalez Lopez, S. Goy Lopez, J.M. Hernandez, M.I. Josa, D. Moran, A. Pérez-Calero Yzquierdo, J. Puerta Pelayo, I. Redondo, L. Romero, M.S. Soares, A. Triossi

Universidad Autónoma de Madrid, Madrid, Spain

C. Albajar, J.F. de Trocóniz

Universidad de Oviedo, Oviedo, Spain

J. Cuevas, C. Erice, J. Fernandez Menendez, S. Folgueras, I. Gonzalez Caballero, J.R. González Fernández, E. Palencia Cortezon, V. Rodríguez Bouza, S. Sanchez Cruz, P. Vischia, J.M. Vizan Garcia

Instituto de Física de Cantabria (IFCA), CSIC-Universidad de Cantabria, Santander, Spain

I.J. Cabrillo, A. Calderon, B. Chazin Quero, J. Duarte Campderros, M. Fernandez, P.J. Fernández Manteca, A. García Alonso, J. Garcia-Ferrero, G. Gomez, A. Lopez Virto, J. Marco, C. Martinez Rivero, P. Martinez Ruiz del Arbol, F. Matorras, J. Piedra Gomez, C. Prieels, T. Rodrigo, A. Ruiz-Jimeno, L. Scodellaro, N. Trevisani, I. Vila, R. Vilar Cortabitarte

University of Ruhuna, Department of Physics, Matara, Sri Lanka

N. Wickramage

CERN, European Organization for Nuclear Research, Geneva, Switzerland

D. Abbaneo, B. Akgun, E. Auffray, G. Auzinger, P. Baillon, A.H. Ball, D. Barney, J. Bendavid, M. Bianco, A. Bocci, C. Botta, E. Brondolin, T. Camporesi, M. Cepeda, G. Cerminara, E. Chapon, Y. Chen, G. Cucciati, D. d'Enterria, A. Dabrowski, N. Daci, V. Daponte, A. David, A. De Roeck, N. Deelen, M. Dobson, M. Dünser, N. Dupont, A. Elliott-Peisert, P. Everaerts, F. Fallavollita[43], D. Fasanella, G. Franzoni, J. Fulcher, W. Funk, D. Gigi, A. Gilbert, K. Gill, F. Glege, M. Gruchala, M. Guilbaud, D. Gulhan, J. Hegeman, C. Heidegger, V. Innocente, A. Jafari, P. Janot, O. Karacheban[18], J. Kieseler, A. Kornmayer, M. Krammer[1], C. Lange, P. Lecoq, C. Lourenço, L. Malgeri, M. Mannelli, F. Meijers, J.A. Merlin, S. Mersi, E. Meschi, P. Milenovic[44], F. Moortgat, M. Mulders, J. Ngadiuba, S. Nourbakhsh, S. Orfanelli, L. Orsini, F. Pantaleo[15], L. Pape, E. Perez, M. Peruzzi, A. Petrilli, G. Petrucciani, A. Pfeiffer, M. Pierini, F.M. Pitters, D. Rabady, A. Racz, T. Reis, M. Rovere, H. Sakulin, C. Schäfer, C. Schwick, M. Seidel, M. Selvaggi,

A. Sharma, P. Silva, P. Sphicas[45], A. Stakia, J. Steggemann, D. Treille, A. Tsirou, V. Veckalns[46], M. Verzetti, W.D. Zeuner

Paul Scherrer Institut, Villigen, Switzerland

L. Caminada[47], K. Deiters, W. Erdmann, R. Horisberger, Q. Ingram, H.C. Kaestli, D. Kotlinski, U. Langenegger, T. Rohe, S.A. Wiederkehr

ETH Zurich — Institute for Particle Physics and Astrophysics (IPA), Zurich, Switzerland

M. Backhaus, L. Bäni, P. Berger, N. Chernyavskaya, G. Dissertori, M. Dittmar, M. Donegà, C. Dorfer, T.A. Gómez Espinosa, C. Grab, D. Hits, T. Klijnsma, W. Lustermann, R.A. Manzoni, M. Marionneau, M.T. Meinhard, F. Micheli, P. Musella, F. Nessi-Tedaldi, J. Pata, F. Pauss, G. Perrin, L. Perrozzi, S. Pigazzini, M. Quittnat, C. Reissel, D. Ruini, D.A. Sanz Becerra, M. Schönenberger, L. Shchutska, V.R. Tavolaro, K. Theofilatos, M.L. Vesterbacka Olsson, R. Wallny, D.H. Zhu

Universität Zürich, Zurich, Switzerland

T.K. Aarrestad, C. Amsler[48], D. Brzhechko, M.F. Canelli, A. De Cosa, R. Del Burgo, S. Donato, C. Galloni, T. Hreus, B. Kilminster, S. Leontsinis, I. Neutelings, G. Rauco, P. Robmann, D. Salerno, K. Schweiger, C. Seitz, Y. Takahashi, A. Zucchetta

National Central University, Chung-Li, Taiwan

Y.H. Chang, K.y. Cheng, T.H. Doan, R. Khurana, C.M. Kuo, W. Lin, A. Pozdnyakov, S.S. Yu

National Taiwan University (NTU), Taipei, Taiwan

P. Chang, Y. Chao, K.F. Chen, P.H. Chen, W.-S. Hou, Arun Kumar, Y.F. Liu, R.-S. Lu, E. Paganis, A. Psallidas, A. Steen

Chulalongkorn University, Faculty of Science, Department of Physics, Bangkok, Thailand

B. Asavapibhop, N. Srimanobhas, N. Suwonjandee

Çukurova University, Physics Department, Science and Art Faculty, Adana, Turkey

A. Bat, F. Boran, S. Cerci[49], S. Damarseckin, Z.S. Demiroglu, F. Dolek, C. Dozen, I. Dumanoglu, E. Eskut, S. Girgis, G. Gokbulut, Y. Guler, E. Gurpinar, I. Hos[50], C. Isik, E.E. Kangal[51], O. Kara, A. Kayis Topaksu, U. Kiminsu, M. Oglakci, G. Onengut, K. Ozdemir[52], A. Polatoz, B. Tali[49], U.G. Tok, S. Turkcapar, I.S. Zorbakir, C. Zorbilmez

Middle East Technical University, Physics Department, Ankara, Turkey

B. Isildak[53], G. Karapinar[54], M. Yalvac, M. Zeyrek

Bogazici University, Istanbul, Turkey

I.O. Atakisi, E. Gülmez, M. Kaya[55], O. Kaya[56], S. Ozkorucuklu[57], S. Tekten, E.A. Yetkin[58]

Istanbul Technical University, Istanbul, Turkey

M.N. Agaras, A. Cakir, K. Cankocak, Y. Komurcu, S. Sen[59]

Institute for Scintillation Materials of National Academy of Science of Ukraine, Kharkov, Ukraine

B. Grynyov

National Scientific Center, Kharkov Institute of Physics and Technology, Kharkov, Ukraine

L. Levchuk

University of Bristol, Bristol, United Kingdom

F. Ball, L. Beck, J.J. Brooke, D. Burns, E. Clement, D. Cussans, O. Davignon, H. Flacher, J. Goldstein, G.P. Heath, H.F. Heath, L. Kreczko, D.M. Newbold[60], S. Paramesvaran, B. Penning, T. Sakuma, D. Smith, V.J. Smith, J. Taylor, A. Titterton

Rutherford Appleton Laboratory, Didcot, United Kingdom

K.W. Bell, A. Belyaev[61], C. Brew, R.M. Brown, D. Cieri, D.J.A. Cockerill, J.A. Coughlan, K. Harder, S. Harper, J. Linacre, E. Olaiya, D. Petyt, C.H. Shepherd-Themistocleous, A. Thea, I.R. Tomalin, T. Williams, W.J. Womersley

Imperial College, London, United Kingdom

R. Bainbridge, P. Bloch, J. Borg, S. Breeze, O. Buchmuller, A. Bundock, D. Colling, P. Dauncey, G. Davies, M. Della Negra, R. Di Maria, G. Hall, G. Iles, T. James, M. Komm, C. Laner, L. Lyons, A.-M. Magnan, S. Malik, A. Martelli, J. Nash[62], A. Nikitenko[7], V. Palladino, M. Pesaresi, D.M. Raymond, A. Richards, A. Rose, E. Scott, C. Seez, A. Shtipliyski, G. Singh, M. Stoye, T. Strebler, S. Summers, A. Tapper, K. Uchida, T. Virdee[15], N. Wardle, D. Winterbottom, J. Wright, S.C. Zenz

Brunel University, Uxbridge, United Kingdom

J.E. Cole, P.R. Hobson, A. Khan, P. Kyberd, C.K. Mackay, A. Morton, I.D. Reid, L. Teodorescu, S. Zahid

Baylor University, Waco, U.S.A.

K. Call, J. Dittmann, K. Hatakeyama, H. Liu, C. Madrid, B. McMaster, N. Pastika, C. Smith

Catholic University of America, Washington DC, U.S.A.

R. Bartek, A. Dominguez

The University of Alabama, Tuscaloosa, U.S.A.

A. Buccilli, S.I. Cooper, C. Henderson, P. Rumerio, C. West

Boston University, Boston, U.S.A.

D. Arcaro, T. Bose, D. Gastler, D. Pinna, D. Rankin, C. Richardson, J. Rohlf, L. Sulak, D. Zou

Brown University, Providence, U.S.A.

G. Benelli, X. Coubez, D. Cutts, M. Hadley, J. Hakala, U. Heintz, J.M. Hogan[63], K.H.M. Kwok, E. Laird, G. Landsberg, J. Lee, Z. Mao, M. Narain, S. Sagir[64], R. Syarif, E. Usai, D. Yu

University of California, Davis, Davis, U.S.A.

R. Band, C. Brainerd, R. Breedon, D. Burns, M. Calderon De La Barca Sanchez, M. Chertok, J. Conway, R. Conway, P.T. Cox, R. Erbacher, C. Flores, G. Funk, W. Ko, O. Kukral, R. Lander, M. Mulhearn, D. Pellett, J. Pilot, S. Shalhout, M. Shi, D. Stolp, D. Taylor, K. Tos, M. Tripathi, Z. Wang, F. Zhang

University of California, Los Angeles, U.S.A.

M. Bachtis, C. Bravo, R. Cousins, A. Dasgupta, A. Florent, J. Hauser, M. Ignatenko, N. Mccoll, S. Regnard, D. Saltzberg, C. Schnaible, V. Valuev

University of California, Riverside, Riverside, U.S.A.

E. Bouvier, K. Burt, R. Clare, J.W. Gary, S.M.A. Ghiasi Shirazi, G. Hanson, G. Karapostoli, E. Kennedy, F. Lacroix, O.R. Long, M. Olmedo Negrete, M.I. Paneva, W. Si, L. Wang, H. Wei, S. Wimpenny, B.R. Yates

University of California, San Diego, La Jolla, U.S.A.

J.G. Branson, P. Chang, S. Cittolin, M. Derdzinski, R. Gerosa, D. Gilbert, B. Hashemi, A. Holzner, D. Klein, G. Kole, V. Krutelyov, J. Letts, M. Masciovecchio, D. Olivito, S. Padhi, M. Pieri, M. Sani, V. Sharma, S. Simon, M. Tadel, A. Vartak, S. Wasserbaech[65], J. Wood, F. Würthwein, A. Yagil, G. Zevi Della Porta

University of California, Santa Barbara — Department of Physics, Santa Barbara, U.S.A.

N. Amin, R. Bhandari, J. Bradmiller-Feld, C. Campagnari, M. Citron, A. Dishaw, V. Dutta, M. Franco Sevilla, L. Gouskos, R. Heller, J. Incandela, A. Ovcharova, H. Qu, J. Richman, D. Stuart, I. Suarez, S. Wang, J. Yoo

California Institute of Technology, Pasadena, U.S.A.

D. Anderson, A. Bornheim, J.M. Lawhorn, N. Lu, H.B. Newman, T.Q. Nguyen, M. Spiropulu, J.R. Vlimant, R. Wilkinson, S. Xie, Z. Zhang, R.Y. Zhu

Carnegie Mellon University, Pittsburgh, U.S.A.

M.B. Andrews, T. Ferguson, T. Mudholkar, M. Paulini, M. Sun, I. Vorobiev, M. Weinberg

University of Colorado Boulder, Boulder, U.S.A.

J.P. Cumalat, W.T. Ford, F. Jensen, A. Johnson, M. Krohn, E. MacDonald, T. Mulholland, R. Patel, A. Perloff, K. Stenson, K.A. Ulmer, S.R. Wagner

Cornell University, Ithaca, U.S.A.

J. Alexander, J. Chaves, Y. Cheng, J. Chu, A. Datta, K. Mcdermott, N. Mirman, J.R. Patterson, D. Quach, A. Rinkevicius, A. Ryd, L. Skinnari, L. Soffi, S.M. Tan, Z. Tao, J. Thom, J. Tucker, P. Wittich, M. Zientek

Fermi National Accelerator Laboratory, Batavia, U.S.A.

S. Abdullin, M. Albrow, M. Alyari, G. Apollinari, A. Apresyan, A. Apyan, S. Banerjee, L.A.T. Bauerdick, A. Beretvas, J. Berryhill, P.C. Bhat, K. Burkett, J.N. Butler, A. Canepa, G.B. Cerati, H.W.K. Cheung, F. Chlebana, M. Cremonesi, J. Duarte, V.D. Elvira, J. Freeman, Z. Gecse, E. Gottschalk, L. Gray, D. Green, S. Grünendahl, O. Gutsche,

J. Hanlon, R.M. Harris, S. Hasegawa, J. Hirschauer, Z. Hu, B. Jayatilaka, S. Jindariani, M. Johnson, U. Joshi, B. Klima, M.J. Kortelainen, B. Kreis, S. Lammel, D. Lincoln, R. Lipton, M. Liu, T. Liu, J. Lykken, K. Maeshima, J.M. Marraffino, D. Mason, P. McBride, P. Merkel, S. Mrenna, S. Nahn, V. O'Dell, K. Pedro, C. Pena, O. Prokofyev, G. Rakness, L. Ristori, A. Savoy-Navarro[66], B. Schneider, E. Sexton-Kennedy, A. Soha, W.J. Spalding, L. Spiegel, S. Stoynev, J. Strait, N. Strobbe, L. Taylor, S. Tkaczyk, N.V. Tran, L. Uplegger, E.W. Vaandering, C. Vernieri, M. Verzocchi, R. Vidal, M. Wang, H.A. Weber, A. Whitbeck

University of Florida, Gainesville, U.S.A.

D. Acosta, P. Avery, P. Bortignon, D. Bourilkov, A. Brinkerhoff, L. Cadamuro, A. Carnes, D. Curry, R.D. Field, S.V. Gleyzer, B.M. Joshi, J. Konigsberg, A. Korytov, K.H. Lo, P. Ma, K. Matchev, H. Mei, G. Mitselmakher, D. Rosenzweig, K. Shi, D. Sperka, J. Wang, S. Wang, X. Zuo

Florida International University, Miami, U.S.A.

Y.R. Joshi, S. Linn

Florida State University, Tallahassee, U.S.A.

A. Ackert, T. Adams, A. Askew, S. Hagopian, V. Hagopian, K.F. Johnson, T. Kolberg, G. Martinez, T. Perry, H. Prosper, A. Saha, C. Schiber, R. Yohay

Florida Institute of Technology, Melbourne, U.S.A.

M.M. Baarmand, V. Bhopatkar, S. Colafranceschi, M. Hohlmann, D. Noonan, M. Rahmani, T. Roy, F. Yumiceva

University of Illinois at Chicago (UIC), Chicago, U.S.A.

M.R. Adams, L. Apanasevich, D. Berry, R.R. Betts, R. Cavanaugh, X. Chen, S. Dittmer, O. Evdokimov, C.E. Gerber, D.A. Hangal, D.J. Hofman, K. Jung, J. Kamin, C. Mills, I.D. Sandoval Gonzalez, M.B. Tonjes, H. Trauger, N. Varelas, H. Wang, X. Wang, Z. Wu, J. Zhang

The University of Iowa, Iowa City, U.S.A.

M. Alhusseini, B. Bilki[67], W. Clarida, K. Dilsiz[68], S. Durgut, R.P. Gandrajula, M. Haytmyradov, V. Khristenko, J.-P. Merlo, A. Mestvirishvili, A. Moeller, J. Nachtman, H. Ogul[69], Y. Onel, F. Ozok[70], A. Penzo, C. Snyder, E. Tiras, J. Wetzel

Johns Hopkins University, Baltimore, U.S.A.

B. Blumenfeld, A. Cocoros, N. Eminizer, D. Fehling, L. Feng, A.V. Gritsan, W.T. Hung, P. Maksimovic, J. Roskes, U. Sarica, M. Swartz, M. Xiao, C. You

The University of Kansas, Lawrence, U.S.A.

A. Al-bataineh, P. Baringer, A. Bean, S. Boren, J. Bowen, A. Bylinkin, J. Castle, S. Khalil, A. Kropivnitskaya, D. Majumder, W. Mcbrayer, M. Murray, C. Rogan, S. Sanders, E. Schmitz, J.D. Tapia Takaki, Q. Wang

Kansas State University, Manhattan, U.S.A.

S. Duric, A. Ivanov, K. Kaadze, D. Kim, Y. Maravin, D.R. Mendis, T. Mitchell, A. Modak, A. Mohammadi, L.K. Saini, N. Skhirtladze

Lawrence Livermore National Laboratory, Livermore, U.S.A.

F. Rebassoo, D. Wright

University of Maryland, College Park, U.S.A.

A. Baden, O. Baron, A. Belloni, S.C. Eno, Y. Feng, C. Ferraioli, N.J. Hadley, S. Jabeen, G.Y. Jeng, R.G. Kellogg, J. Kunkle, A.C. Mignerey, S. Nabili, F. Ricci-Tam, Y.H. Shin, A. Skuja, S.C. Tonwar, K. Wong

Massachusetts Institute of Technology, Cambridge, U.S.A.

D. Abercrombie, B. Allen, V. Azzolini, A. Baty, G. Bauer, R. Bi, S. Brandt, W. Busza, I.A. Cali, M. D'Alfonso, Z. Demiragli, G. Gomez Ceballos, M. Goncharov, P. Harris, D. Hsu, M. Hu, Y. Iiyama, G.M. Innocenti, M. Klute, D. Kovalskyi, Y.-J. Lee, P.D. Luckey, B. Maier, A.C. Marini, C. Mcginn, C. Mironov, S. Narayanan, X. Niu, C. Paus, C. Roland, G. Roland, G.S.F. Stephans, K. Sumorok, K. Tatar, D. Velicanu, J. Wang, T.W. Wang, B. Wyslouch, S. Zhaozhong

University of Minnesota, Minneapolis, U.S.A.

A.C. Benvenuti[†], R.M. Chatterjee, A. Evans, P. Hansen, J. Hiltbrand, Sh. Jain, S. Kalafut, Y. Kubota, Z. Lesko, J. Mans, N. Ruckstuhl, R. Rusack, M.A. Wadud

University of Mississippi, Oxford, U.S.A.

J.G. Acosta, S. Oliveros

University of Nebraska-Lincoln, Lincoln, U.S.A.

E. Avdeeva, K. Bloom, D.R. Claes, C. Fangmeier, F. Golf, R. Gonzalez Suarez, R. Kamalieddin, I. Kravchenko, J. Monroy, J.E. Siado, G.R. Snow, B. Stieger

State University of New York at Buffalo, Buffalo, U.S.A.

A. Godshalk, C. Harrington, I. Iashvili, A. Kharchilava, C. Mclean, D. Nguyen, A. Parker, S. Rappoccio, B. Roozbahani

Northeastern University, Boston, U.S.A.

G. Alverson, E. Barberis, C. Freer, Y. Haddad, A. Hortiangtham, D.M. Morse, T. Orimoto, R. Teixeira De Lima, T. Wamorkar, B. Wang, A. Wisecarver, D. Wood

Northwestern University, Evanston, U.S.A.

S. Bhattacharya, J. Bueghly, O. Charaf, K.A. Hahn, N. Mucia, N. Odell, M.H. Schmitt, K. Sung, M. Trovato, M. Velasco

University of Notre Dame, Notre Dame, U.S.A.

R. Bucci, N. Dev, M. Hildreth, K. Hurtado Anampa, C. Jessop, D.J. Karmgard, N. Kellams, K. Lannon, W. Li, N. Loukas, N. Marinelli, F. Meng, C. Mueller, Y. Musienko[35], M. Planer, A. Reinsvold, R. Ruchti, P. Siddireddy, G. Smith, S. Taroni, M. Wayne, A. Wightman, M. Wolf, A. Woodard

The Ohio State University, Columbus, U.S.A.

J. Alimena, L. Antonelli, B. Bylsma, L.S. Durkin, S. Flowers, B. Francis, C. Hill, W. Ji, T.Y. Ling, W. Luo, B.L. Winer

Princeton University, Princeton, U.S.A.

S. Cooperstein, P. Elmer, J. Hardenbrook, S. Higginbotham, A. Kalogeropoulos, D. Lange, M.T. Lucchini, J. Luo, D. Marlow, K. Mei, I. Ojalvo, J. Olsen, C. Palmer, P. Piroué, J. Salfeld-Nebgen, D. Stickland, C. Tully

University of Puerto Rico, Mayaguez, U.S.A.

S. Malik, S. Norberg

Purdue University, West Lafayette, U.S.A.

A. Barker, V.E. Barnes, S. Das, L. Gutay, M. Jones, A.W. Jung, A. Khatiwada, B. Mahakud, D.H. Miller, N. Neumeister, C.C. Peng, S. Piperov, H. Qiu, J.F. Schulte, J. Sun, F. Wang, R. Xiao, W. Xie

Purdue University Northwest, Hammond, U.S.A.

T. Cheng, J. Dolen, N. Parashar

Rice University, Houston, U.S.A.

Z. Chen, K.M. Ecklund, S. Freed, F.J.M. Geurts, M. Kilpatrick, W. Li, B.P. Padley, J. Roberts, J. Rorie, W. Shi, Z. Tu, A. Zhang

University of Rochester, Rochester, U.S.A.

A. Bodek, P. de Barbaro, R. Demina, Y.t. Duh, J.L. Dulemba, C. Fallon, T. Ferbel, M. Galanti, A. Garcia-Bellido, J. Han, O. Hindrichs, A. Khukhunaishvili, E. Ranken, P. Tan, R. Taus

Rutgers, The State University of New Jersey, Piscataway, U.S.A.

A. Agapitos, J.P. Chou, Y. Gershtein, E. Halkiadakis, A. Hart, M. Heindl, E. Hughes, S. Kaplan, R. Kunnawalkam Elayavalli, S. Kyriacou, A. Lath, R. Montalvo, K. Nash, M. Osherson, H. Saka, S. Salur, S. Schnetzer, D. Sheffield, S. Somalwar, R. Stone, S. Thomas, P. Thomassen, M. Walker

University of Tennessee, Knoxville, U.S.A.

A.G. Delannoy, J. Heideman, G. Riley, S. Spanier

Texas A&M University, College Station, U.S.A.

O. Bouhali[71], A. Celik, M. Dalchenko, M. De Mattia, A. Delgado, S. Dildick, R. Eusebi, J. Gilmore, T. Huang, T. Kamon[72], S. Luo, R. Mueller, D. Overton, L. Perniè, D. Rathjens, A. Safonov

Texas Tech University, Lubbock, U.S.A.

N. Akchurin, J. Damgov, F. De Guio, P.R. Dudero, S. Kunori, K. Lamichhane, S.W. Lee, T. Mengke, S. Muthumuni, T. Peltola, S. Undleeb, I. Volobouev, Z. Wang

Vanderbilt University, Nashville, U.S.A.

S. Greene, A. Gurrola, R. Janjam, W. Johns, C. Maguire, A. Melo, H. Ni, K. Padeken, J.D. Ruiz Alvarez, P. Sheldon, S. Tuo, J. Velkovska, M. Verweij, Q. Xu

University of Virginia, Charlottesville, U.S.A.

M.W. Arenton, P. Barria, B. Cox, R. Hirosky, M. Joyce, A. Ledovskoy, H. Li, C. Neu, T. Sinthuprasith, Y. Wang, E. Wolfe, F. Xia

Wayne State University, Detroit, U.S.A.

R. Harr, P.E. Karchin, N. Poudyal, J. Sturdy, P. Thapa, S. Zaleski

University of Wisconsin — Madison, Madison, WI, U.S.A.

M. Brodski, J. Buchanan, C. Caillol, D. Carlsmith, S. Dasu, I. De Bruyn, L. Dodd, B. Gomber, M. Grothe, M. Herndon, A. Hervé, U. Hussain, P. Klabbers, A. Lanaro, K. Long, R. Loveless, T. Ruggles, A. Savin, V. Sharma, N. Smith, W.H. Smith, N. Woods

† : Deceased
1: Also at Vienna University of Technology, Vienna, Austria
2: Also at IRFU, CEA, Université Paris-Saclay, Gif-sur-Yvette, France
3: Also at Universidade Estadual de Campinas, Campinas, Brazil
4: Also at Federal University of Rio Grande do Sul, Porto Alegre, Brazil
5: Also at Université Libre de Bruxelles, Bruxelles, Belgium
6: Also at University of Chinese Academy of Sciences, Beijing, China
7: Also at Institute for Theoretical and Experimental Physics, Moscow, Russia
8: Also at Joint Institute for Nuclear Research, Dubna, Russia
9: Also at Suez University, Suez, Egypt
10: Now at British University in Egypt, Cairo, Egypt
11: Also at Zewail City of Science and Technology, Zewail, Egypt
12: Also at Department of Physics, King Abdulaziz University, Jeddah, Saudi Arabia
13: Also at Université de Haute Alsace, Mulhouse, France
14: Also at Skobeltsyn Institute of Nuclear Physics, Lomonosov Moscow State University, Moscow, Russia
15: Also at CERN, European Organization for Nuclear Research, Geneva, Switzerland
16: Also at RWTH Aachen University, III. Physikalisches Institut A, Aachen, Germany
17: Also at University of Hamburg, Hamburg, Germany
18: Also at Brandenburg University of Technology, Cottbus, Germany
19: Also at MTA-ELTE Lendület CMS Particle and Nuclear Physics Group, Eötvös Loránd University, Budapest, Hungary
20: Also at Institute of Nuclear Research ATOMKI, Debrecen, Hungary
21: Also at Institute of Physics, University of Debrecen, Debrecen, Hungary
22: Also at Indian Institute of Technology Bhubaneswar, Bhubaneswar, India
23: Also at Institute of Physics, Bhubaneswar, India
24: Also at Shoolini University, Solan, India
25: Also at University of Visva-Bharati, Santiniketan, India
26: Also at Isfahan University of Technology, Isfahan, Iran
27: Also at Plasma Physics Research Center, Science and Research Branch, Islamic Azad University, Tehran, Iran
28: Also at Università degli Studi di Siena, Siena, Italy
29: Also at Scuola Normale e Sezione dell'INFN, Pisa, Italy
30: Also at Kyunghee University, Seoul, Korea
31: Also at International Islamic University of Malaysia, Kuala Lumpur, Malaysia
32: Also at Malaysian Nuclear Agency, MOSTI, Kajang, Malaysia

33: Also at Consejo Nacional de Ciencia y Tecnología, Mexico city, Mexico

34: Also at Warsaw University of Technology, Institute of Electronic Systems, Warsaw, Poland

35: Also at Institute for Nuclear Research, Moscow, Russia

36: Now at National Research Nuclear University 'Moscow Engineering Physics Institute' (MEPhI), Moscow, Russia

37: Also at St. Petersburg State Polytechnical University, St. Petersburg, Russia

38: Also at University of Florida, Gainesville, U.S.A.

39: Also at P.N. Lebedev Physical Institute, Moscow, Russia

40: Also at California Institute of Technology, Pasadena, U.S.A.

41: Also at Budker Institute of Nuclear Physics, Novosibirsk, Russia

42: Also at Faculty of Physics, University of Belgrade, Belgrade, Serbia

43: Also at INFN Sezione di Pavia ^{a}, Università di Pavia ^{b}, Pavia, Italy

44: Also at University of Belgrade, Faculty of Physics and Vinca Institute of Nuclear Sciences, Belgrade, Serbia

45: Also at National and Kapodistrian University of Athens, Athens, Greece

46: Also at Riga Technical University, Riga, Latvia

47: Also at Universität Zürich, Zurich, Switzerland

48: Also at Stefan Meyer Institute for Subatomic Physics (SMI), Vienna, Austria

49: Also at Adiyaman University, Adiyaman, Turkey

50: Also at Istanbul Aydin University, Istanbul, Turkey

51: Also at Mersin University, Mersin, Turkey

52: Also at Piri Reis University, Istanbul, Turkey

53: Also at Ozyegin University, Istanbul, Turkey

54: Also at Izmir Institute of Technology, Izmir, Turkey

55: Also at Marmara University, Istanbul, Turkey

56: Also at Kafkas University, Kars, Turkey

57: Also at Istanbul University, Faculty of Science, Istanbul, Turkey

58: Also at Istanbul Bilgi University, Istanbul, Turkey

59: Also at Hacettepe University, Ankara, Turkey

60: Also at Rutherford Appleton Laboratory, Didcot, United Kingdom

61: Also at School of Physics and Astronomy, University of Southampton, Southampton, United Kingdom

62: Also at Monash University, Faculty of Science, Clayton, Australia

63: Also at Bethel University, St. Paul, U.S.A.

64: Also at Karamanoğlu Mehmetbey University, Karaman, Turkey

65: Also at Utah Valley University, Orem, U.S.A.

66: Also at Purdue University, West Lafayette, U.S.A.

67: Also at Beykent University, Istanbul, Turkey

68: Also at Bingol University, Bingol, Turkey

69: Also at Sinop University, Sinop, Turkey

70: Also at Mimar Sinan University, Istanbul, Istanbul, Turkey

71: Also at Texas A&M University at Qatar, Doha, Qatar

72: Also at Kyungpook National University, Daegu, Korea